World Scientific
www.worldscientific.com

Recent Advances of the Constitutive Models of Smart Materials — Hydrogels and Shape Memory Polymers

Rong Huang[*], Shoujing Zheng[*], Zishun Liu[*,‡] and Teng Yong Ng[†]

[*]*International Center for Applied Mechanics*
State Key Laboratory for Strength and
Vibration of Mechanical Structures
Xi'an Jiaotong University, Xi'an 710049, P. R. China

[†]*School of Mechanical and Aerospace Engineering*
Nanyang Technological University, 50 Nanyang Avenue
Singapore 639798, Singapore
[‡]*zishunliu@mail.xjtu.edu.cn*

Hydrogels and shape memory polymers (SMPs) possess excellent and interesting properties that may be harnessed for future applications. However, this is not achievable if their mechanical behaviors are not well understood. This paper aims to discuss recent advances of the constitutive models of hydrogels and SMPs, in particular the theories associated with their deformations. On the one hand, constitutive models of six main types of hydrogels are introduced, the categorization of which is defined by the type of stimulus. On the other hand, constitutive models of thermal-induced SMPs are discussed and classified into three main categories, namely, rheological models; phase transition models; and models combining viscoelasticity and phase transition, respectively. Another feature in this paper is a summary of the common hyperelastic models, which can be potentially developed into the constitutive models of hydrogels and SMPs. In addition, the main advantages and disadvantages of these constitutive modes are discussed. In order to provide a compass for researchers involved in the study of mechanics of soft materials, some research gaps and new research directions for hydrogels and SMPs constitutive modes are presented. We hope that this paper can serve as a reference for future hydrogel and SMP studies.

Keywords: Hydrogels; shape memory polymer; constitutive model; stimulus; deformation; phase transition.

1. Introduction

Over the last two decades and especially in recent times, smart materials have attracted immense interest and have been studied intensively worldwide by both intradisciplinary and multidisciplinary research groups. While machines in the engineering field use mostly hard materials, machines in nature often constitute soft matters. Those soft matters, touted to be the next generation smart materials, can be categorized into many different types, such as gels, shape memory polymers (SMPs), dielectric elastomers (DE), liquid crystal elastomers, etc. [Liu *et al.*, 2015]. In this paper, we discuss fundamental principles and recent advances of the constitutive models of two distinctive smart material groups, hydrogels and SMPs, for their wide potential applications.

Inspired by nature, mankind has developed the synthetic material known as the hydrogel. When a solvent comes into contact with the hydrogel, solvent molecules can move into the network of the gel, resulting in a change in volume because of the absorption of solvent molecules. Possessing the remarkable properties of imbibing solvents and large swelling ratios, hydrogels show potential of emerging as one of the next-generation smart materials in future applications [Gong *et al.*, 2003; Hong *et al.*, 2008, 2009; Liu *et al.*, 2010, 2013]. Hydrogel superiority can be found in properties such as high stretchability [Sun *et al.*, 2012], reversible swelling [Xu *et al.*, 2016b], flexibility [Xu *et al.*, 2016a], biocompatibility [Wei *et al.*, 2015] and toughness [Bouklas *et al.*, 2015; Gong, 2010]. Due to these exceptional advantages, hydrogels have been widely applied in drug delivery [Qiu and Park, 2001], tissue engineering [Drury and Mooney, 2003; Nguyen and West, 2002], actuators [Liu and Calvert, 2000; Zhang *et al.*, 2014], matrices for biological studies [Augst *et al.*, 2006], new metamaterials or smart composite materials [He *et al.*, 2017b; Hu *et al.*, 2013, 2014, 2017, 2018b; Zhou *et al.*, 2019], and the list is still growing, limited only by our imagination.

Although so many advantages are possessed by hydrogels, the range of traditional hydrogel applications is often severely limited by their mechanical behaviors such as low fatigue limit and low fracture threshold [Bai *et al.*, 2017; Li *et al.*, 2019; Zhang *et al.*, 2018a,b]. To understand the deformation behaviors of hydrogels, it is imperative to develop appropriate and robust hydrogel constitutive models. In this paper, we discuss recent advances of these constitutive models necessary for the emerging field of soft machines. For decades, the constitutive models of hydrogel have been developed by many research groups worldwide. Based on their different environmental stimulus types, as shown in Fig. 1, those models can be categorized into neutral gels [Chester and Anand, 2010; Hong *et al.*, 2009; Liu *et al.*, 2019b; Toh *et al.*, 2013, 2015], salt concentration-sensitive gels [Wu and Li, 2018; Zheng and Liu, 2019], pH-sensitive gels [Drozdov *et al.*, 2015; Hamzavi *et al.*, 2016; Li *et al.*, 2005; Toh *et al.*, 2014b; Zhang *et al.*, 2012], temperature-sensitive gels [Birgersson *et al.*, 2008; Chester and Anand, 2011; Ding *et al.*, 2016; Drozdov, 2014; Drozdov and Christiansen, 2017], photo-thermal sensitive gels [Toh *et al.*, 2014a, 2016] and
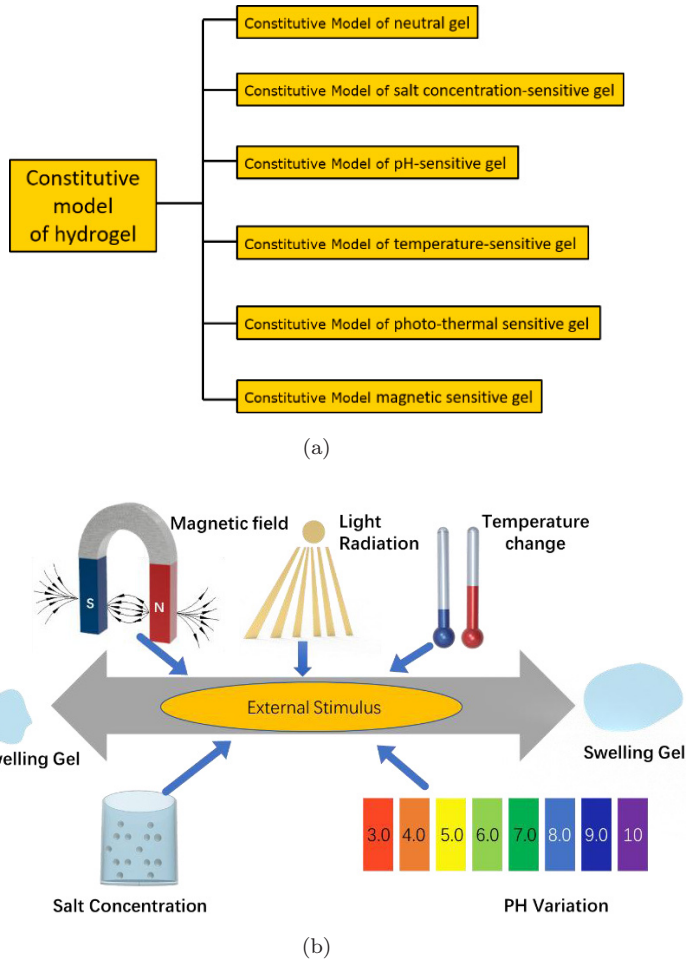
(a)

(b)

Fig. 1. (a) Schematics of different constitutive models of hydrogels and (b) schematics of hydrogels under different external stimuli.

magnetic sensitive gels [Hu *et al.*, 2018a; Liu *et al.*, 2017; Zhao *et al.*, 2019]. These types of stimuli-responsive hydrogels will provide innovative and radical applications over traditional hydrogels. For neutral gels, a type of gel which swells under the stimulus of environmental changes in chemical potential, the constitutive model has been developed by coupling the diffusion and large deformation theory [Chester and Anand, 2010; Hong *et al.*, 2008]. With the same basic formulas of the theories, the constitutive models of other types of hydrogel have also been established. By adding a term of mixing the solvent and ions to the free energy density, the model of the salt concentration-sensitive gel, a type of gel swells under the stimulus of changes in salt concentration inside and outside the gel, has been developed [Liu *et al.*, 2010; Yu *et al.*, 2017; Zheng and Liu, 2019]. Likewise, by considering

dissociating the acidic groups, the model of pH-sensitive hydrogel has been formulated based on the model of salt concentration-sensitive gel [Marcombe *et al.*, 2010; Ng *et al.*, 2007; Toh *et al.*, 2014b]. Also, by introducing fitting parameters into the interaction parameter, the model of the temperature-sensitive gel has been defined [Cai and Suo, 2011; Chester and Anand, 2011; Ding *et al.*, 2013; Drozdov, 2014]. Furthermore, by including the effects of photochemical reaction, the model of the photo-thermal sensitive gel has been attained [Toh *et al.*, 2014a]. Last but not least, by adding a term due to the magnetization, the model of the magnetic sensitive gel has been proposed [Hu *et al.*, 2018a; Liu *et al.*, 2019c; Zhao *et al.*, 2019].

When gels swell in the solvent mixture, two uncommon phenomena may also occur, namely, cosolvency and cononsolvency effects. The former represents gels which can swell more in the mixture than in each individual solvent, while the latter represents good solvents that may become poor solvents when mixed for some specific gels. For the solvent mixture, Xiao *et al.* [2019] developed a constitutive model to describe the equilibrium swelling behaviors of gels in solvent mixtures, which successfully captures experimentally observed cosolvency and cononsolvency effects in different gel-solvent systems. For multiphysics modeling of smart hydrogels, [Li and Lai, 2010; Li *et al.*, 2007a,b,c,d] have theoretically developed several multiphysics models that are able to numerically simulate the multiphase smart soft hydrogels in continuous multi-domain, where the three different phases of hydrogels are considered simultaneously. The multiphysics (coupled chemo-electro-mechanical or higher complexity) fields are included and the performance of the polymeric network solid matrices with flow of ions and interstitial fluid being characterized. These models are in the form of coupled nonlinear partial differential equations for numerical simulation of the fundamental mechanism and performance of the smart hydrogels responsive to the nine kinds of external stimuli in environment solutions, respectively.

In all the above-discussed theories, there are many parameters which are hard to be quantified by continuum mechanics methods, such as solvent chemical potential, molecule size, and the diffusion coefficient of solvent [Xu *et al.*, 2016b]. Furthermore, some of the unusual phenomena observed in experimental studies are hardly described and explained from the macro-level through continuum mechanics [Li and Liu, 2019; Li *et al.*, 2019]. To solve these problems, researchers have further investigated hydrogel swelling behaviors from the nano level and meso level by using molecular dynamics (MD) simulation and other meso mechanics methods. MD simulation can provide detailed structures and dynamical information of the hydrogel system at the molecular level. For example, from molecular level studies, it is found that when the mass fraction of solvent is about 90%, PAAM hydrogel reaches its free swelling limitation and loses its solvent absorbing ability; and that PAAM hydrogel has a phase transition phenomenon when the values of solvent chemical potential are between $-23.4\,\text{kcal/mol}$ and $-20.4\,\text{kcal/mol}$. Furthermore, the thermal conductivities of the PAAM hydrogel with different water volume fractions are investigated at the nanoscale by a nonequilibrium MD method [Xu *et al.*, 2016b, 2018; Xu and Liu, 2019].

Another type of soft matter which has been extensively studied recently is the SMPs. As a class of stimulus responsive smart materials, SMPs have the capability to return to their original (permanent) shape from a programmed temporary shape, with changes in their ambient environment, such as temperature, light, pH values, electricity, etc. Compared to other traditional shape-memory materials including shape memory alloys and shape memory ceramics, SMPs possess several advantages: lightweight, low cost, good biocompatibility and especially large deformation recovery capacity [Baghani *et al.*, 2012; Hager *et al.*, 2015; Leng *et al.*, 2009]. Due to these advantages, some applications have been developed for SMPs' potential uses [He *et al.*, 2015, 2017a, 2018], such as functional textiles [Hu and Chen, 2010], aircraft equipment and aerospace structures [Behl *et al.*, 2010; Hu *et al.*, 2012; Li *et al.*, 2018], self-healing materials [Luo and Mather, 2013; Shojaei *et al.*, 2013], and adaptive biomedical devices [Lendlein *et al.*, 2010; Liu *et al.*, 2019e].

In earlier reported works, several researchers have characterized the shape memory behaviors of SMPs from the perspective of certain specific interests [Liu *et al.*, 2014, 2019d]. However, it is also imperative to establish a comprehensive understanding of the intrinsic mechanisms of SMPs which may limit their potential applications. Therefore, the current review paper will integrate diverse theories by discussing different representative constitutive models, especially for thermal-sensitive SMPs (refer to Fig. 2). Typically, these models can be broadly classified
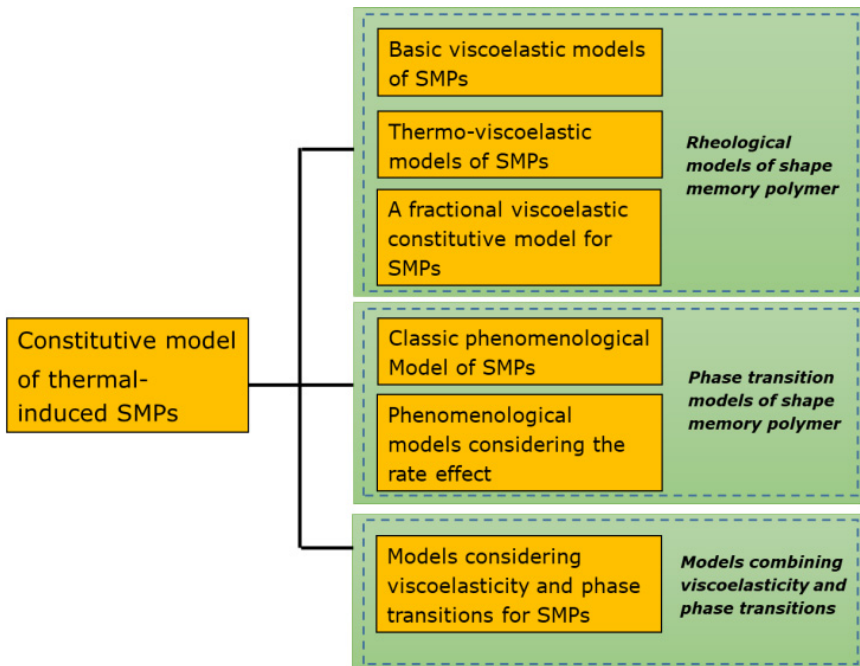

Fig. 2.   Schematics of the constitutive models of thermal-induced SMPs.

into two main categories: rheological models and phenomenological models. The rheological model is based on viscoelastic modeling approaches with rate-dependent and temperature-dependent parameters. The early thermo-viscoelastic constitutive models usually consisted of classical spring and dashpot elements together with the friction modulus which could qualitatively represent the shape memory effect of SMPs. One of the most representative early viscoelastic models was proposed by Tobushi *et al.* [1997, 2001] who introduced an irreversible slip element in the Maxwell spring-damper system to describe the general shape memory process of SMPs. Based on the similar framework of the spring-dashpot system, many other viscoelastic models were subsequently developed and extended to describe the three-dimensional large deformation of SMPs [Diani *et al.*, 2006; Li *et al.*, 2015; Morshedian *et al.*, 2005]. To better characterize the rate-dependent and temperature-dependent performance of amorphous SMPs, researchers have further developed thermo-viscoelastic models with a combination of relaxation behaviors and the viscoelastic behaviors of these SMPs [Castro *et al.*, 2010; Nguyen *et al.*, 2008]. To simplify the prediction process and provide a simple and effective SMP model, [Pan and Liu, 2018] simplified the model parameters with novel fractional viscoelastic constitutive models.

In the study of viscoelastic models for thermally activated shape memory effect (SME), Xiao *et al.* [2015, 2016] formulated a finite deformation viscoelastic model with multiple relaxation processes, which successfully captures the temperature memory effect and multi-shape memory effect in an amorphous polymer Nafion with an extremely broad glass transition region. The model can describe the shape-memory performance of amorphous thermoplastics. Normally, the viscoelastic models cannot be applied to simulate the shape-memory performance of polymers with the temporary shape programmed below the glass transition region. To overcome this limitation, Dai *et al.* [2020] recently developed a viscoplastic model to describe the constrained recovery performance of cold-programmed SMPs. The model successfully captures the dependence of the recovery stress on programming temperature and strain.

Although all previous rheological models could evaluate the thermo-mechanical properties of SMPs and capture the rate and temperature dependence on the SME, they have been unable to relate the phase transition mechanisms to SME and provide clear physical interpretation. Thus, the phenomenological phase transition approach was proposed and has since been extensively studied.

The first phenomenological model of SMPs was introduced by Liu *et al.* [2006], which considered SMPs as a mixture of different phases and the transformation back and forth between these phases could be adjusted by the temperature. Following the same approach, many researchers subsequently provided their own models with distinctive assumptions. [Chen and Lagoudas, 2008a,b] proposed nonlinear constitutive models to represent the large deformation of SMPs, and Qi *et al.* [2008] redefined the glassy phase of SMPs to obtain more accurate three-phase transition models. Lu *et al.* [2019] developed a cooperative domain model to describe

the glass transition and relaxation behaviors of SMPs, particularly to characterize the tripe-SME in multiple phase SMPs. Besides, many other comprehensive phenomenological models have been developed based on the phase transition concept, such as Reese *et al.* [2010], Long *et al.* [2010], Xu and Li [2010], Baghani *et al.* [2014], Gu *et al.* [2015], Moon *et al.* [2015], Yang and Li [2015], Li *et al.* [2017b], Lu *et al.* [2018] and Pan *et al.* [2018]. Previous studies on these phase transition models showed that phenomenological models could provide clear physical interpretation between the glass transition and SME. However, the viscosity and rate dependency effect on the SME is hard to express within this system. Shortly after, researchers attempted to combine both the viscoelasticity and phase transition of SMPs in the constitutive models. Li *et al.* [2017a] proposed a phase-evolution-based thermomechanical constitutive model which can capture the SME of amorphous SMPs with viscoelastic properties of polymers and the phase transition phenomenon. Later, Li and Liu [2018] improved upon this method and proposed a new model which could not only provide an exact prediction of the rate-dependent shape memory behaviors, but also describe the creep and stress relaxation of the SMPs with a clear physical interpretation.

Although SMPs have drawn wide attention in research and application, their low modulus and recovery stress limit their application and thus also their development. Researchers have proposed an approach to improve or reinforce these mechanical properties of SMPs. Pan *et al.* [2019] have studied the mechanical properties and SME of spherical particle reinforced shape memory polymer composite (SMPC) through a representative volume element created by using the random sequential adsorption algorithm. They found that the elastic modulus and recovery stress are increased considerably by adding 15% volume fraction glass beads into the SMP.

With the rapid proliferation of the potential of hydrogels and SMPs in applications in diversified fields, a better perception and understanding of the mechanics of those two smart material groups is crucial. For example, adhesion of soft materials has been extensively studied recently. The hydrogel-SMP hybrids based on adhesion can take advantage of both smart materials, which is worth further investigation. As mentioned above, in the past decade, many relevant constitutive models have been proposed to describe and predict the mechanical behavior of gels and SMPs. With a better understanding of their underlying mechanics, designing more applications with improved mechanical performance can then be achieved.

The paper is organized as follows. Section 2 provides some basic formulations of the theories and some common background knowledge of gels and SMPs. Section 3 covers the constitutive models of hydrogels. Section 4 covers the constitutive models of shape memory polymers. Section 5 discusses the differences between those models. Section 6 investigates potential applications and identifies some research gaps. Concluding remarks are given in Sec. 7.

2. Basic Formulas of Constitutive Models

2.1. *Preliminary formulas of deformation*

For large deformation of hydrogels and SMPs, there are two different states, namely, the reference state, and the current state (or the state of hydrogels and SMPs at time t). We can select any state as the reference state (e.g., take the stress-free dry network for hydrogel) and name each small part of the network in its coordinate $\mathbf{X}$ in the reference state. In a deformed state, this part of the network moves to a place with the coordinate $x_i(\mathbf{X})$. Denote the deformation gradient by

$$F_{iK} = \frac{\partial x_i(X, t)}{\partial X_K} \quad \text{or} \quad \mathbf{F} = \left(\frac{\partial \mathbf{x}(X, t)}{\partial \mathbf{X}} \right)^T. \tag{2.1}$$

In the deformation process, the deformation gradient $\mathbf{F}$ can normally be multiplicative decomposed for different constitutive models. For hydrogel deformation, relative to the dry network, the state of free swelling is characterized by the deformation gradient

$$\mathbf{F}_0 = \begin{bmatrix} \lambda_0 & & \\ & \lambda_0 & \\ & & \lambda_0 \end{bmatrix}. \tag{2.2}$$

Practically, it is often easier to use the initial stress-free state of an isotropically pre swollen gel as the reference. The deformation gradient of the initial state is $\mathbf{F}_0 = \lambda_0 \mathbf{I}$, $\mathbf{I}$ where is identity matrix, and the total deformation gradient in current state can be decomposed into

$$\mathbf{F} = \mathbf{F}' \mathbf{F}_0 \quad \text{or} \quad F = F_d F_0, \tag{2.3}$$

where $\mathbf{F}'$ or $\mathbf{F_d}$ is the gradient of the current state relative to the free-swelling state, and $\det \mathbf{F} = \det \mathbf{F}' \det \mathbf{F}_0 = \lambda_0^3 \det \mathbf{F}'$.

For SMP deformation, during a typical thermomechanical loading cycle, the total deformation gradient $\mathbf{F}$ can be decomposed as the mixture of the mechanical deformation $\mathbf{F}_m$ and the thermal deformation $\mathbf{F}_{\text{th}}$.

$$\mathbf{F} = \mathbf{F}_m \mathbf{F}_{\text{th}}, \tag{2.4}$$

where $\mathbf{F}_{\text{th}}$ is commonly expressed as a function of the thermal expansion coefficient α and the reference temperature. However, based on different considerations of viscoelasticity, the decomposition of the mechanical deformation gradient may be expressed in different ways.

Diani *et al.* [2006] proposed a 3D thermo-viscoelastic model based on the thermodynamic considerations of SMPs to represent the thermo-mechanical behaviors in the context of finite strain. In the model, the deformation gradient is assumed to be the mixture of change in entropy and change in internal energy, and therefore could be multiplicative decomposed into a viscous part and an elastic part on the

rheological basis, and expressed as follows:

$$\begin{cases} \mathbf{F}_m = \mathbf{F}_e & \text{(entropy or elastic branch)} \\ \mathbf{F}_m = \mathbf{F}_e\,\mathbf{F}_v & \text{(internal energy or viscoelastic branch)} \end{cases}. \tag{2.5}$$

Li *et al.* [2017a] proposed a novel phase transition-based viscoelastic model based on the complicated multiplicative decomposition of the deformation gradient. In rubbery phase, two incompressible hyperplastic elements and one viscous damper were introduced to represent the viscoelastic behaviors of SMPs. As for the glassy phase, the deformation is assumed as a combination of the rubbery phase branch and a reversible phase branch due to the secondary network at low temperature which is expressed as a standard Maxwell spring-dashpot system. The total mechanical deformation gradient $\mathbf{F}_m$ should be accordingly classified in different expressions:

For rubbery phase,

$$\mathbf{F}_m = \mathbf{F}_{H1}\mathbf{F}_{V1} = \mathbf{F}_{H2} \quad (T > Tg). \tag{2.6}$$

For glass phase,

$$\left.\begin{array}{l} \mathbf{F}_m = \mathbf{F}_{m-T_g}\mathbf{F}_{\text{reversible}} \\ \mathbf{F}_{\text{reversible}} = \mathbf{F}_{E2}\mathbf{F}_{V2} = \mathbf{F}_{E1} \end{array}\right\} \quad (T \leq Tg), \tag{2.7}$$

where the subscripts H_1, H_2, E_1, E_2, V_1 and V_2 all represent the corresponding hyperplastic, elastic and viscous elements of the model. $\mathbf{F}_{\text{reversible}}$ denotes the deformation gradient for glassy phase, the deformation gradient of a new formed secondary cross-link is assumed in a stress-free configuration, which means $\mathbf{F}_{\text{reversible}} = 1$ at T_g. The total mechanical deformation $\mathbf{F}_m$ can therefore be correlated with $\mathbf{F}_{\text{reversible}}$ through a given value $\mathbf{F}_{m-T_g}$, which refers to the mechanical deformation at T_g.

2.2. *Equilibrium condition in variational forms*

In order to understand the large deformation of hydrogels, especially their mechanical behaviors, the basic formulas of the large deformation theory are required to be introduced. Hydrogels differ by their stimulus, but a generalized theory has been developed to specify different kinds of hydrogels, including neutral gel, salt concentration-sensitive gel, pH-sensitive gel, temperature-sensitive gel, photothermal sensitive gel and magnetic sensitive gel. Their theories are distinctive in their respective models, but the basic formulas are the same.

Referring to Fig. 3, a gel is subjected to geometrical constraints and attached to a body force P_i and traction T_i is maintained at chemical potential μ. It should be noted that different types of hydrogels may be subjected to more different physical constrains. For example, in the case of magnetic sensitive gel, there should be a wire nearby, alternating the current I, inducing a magnetic field B in the gel. The work done on the gel by the mechanical load and solvent are $P\delta l$ and $\mu\delta N$, respectively.
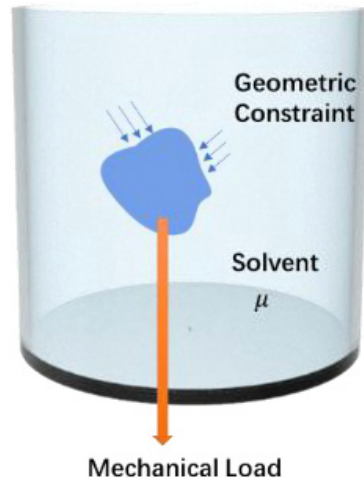
Fig. 3. A gel is in contact with a solvent of a fixed chemical potential, and is subject to a mechanical load and a geometric constraint.

It should also be noted that different types of hydrogels may carry out different forms of work done. For example, the work done by magnetic sensitive gel through the magnetic field $B\delta M$ should be added to the system.

For basic formulas that can be applied to all types of hydrogels, the work done on the gel causes a change in the free energy density of the system

$$\int \delta W dV = \int B_i \delta x_i dV + \int T_i \delta x_i dS + \mu \int \delta C dV. \tag{2.8}$$

Using the deformation gradient as a measure of amount of deformation and introducing the divergence theorem, Eq. (2.8) is rewritten as

$$\int \delta W dV = \int s_{iK} \delta F_{iK} dV + \mu \int \delta C dV. \tag{2.9}$$

Writing the change in free energy density using the chain rule of partial derivatives, we can obtain

$$\int \left(\frac{\partial W}{\partial F_{iK}} \delta F_{iK} + \frac{\partial W}{\partial C} \delta C \right) dV = \int s_{iK} \delta F_{iK} dV + \mu \int \delta C dV, \tag{2.10}$$

under the assumption that the free energy density is a variable dependent on the state of deformation and the solvent concentration.

For arbitrary values of the integrand, Eq. (2.10) reduces to the set of two differential equations

$$s_{iK} = \frac{\partial W}{\partial F_{iK}}, \quad \mu = \frac{\partial W}{\partial C}. \tag{2.11}$$

The next step is to define the free energy density W. Following Flory and Rehner [1943], for basic formulas of the theory, we assume that the total free energy density

can be decomposed into a linear sum of the two component densities

$$W(F_{iK}, C) = W_{\text{str}}(F_{iK}) + W_{\text{mix}}(C). \tag{2.12}$$

For different types of hydrogels, different types of energy densities can be added to Eq. (2.12).

In Eq. (2.12), the free energy density of network stretch is taken to be of Gaussian form, which is given by [Flory, 1953]

$$W_{\text{str}} = \frac{1}{2}NkT[\mathbf{F} : \mathbf{F} - 3 - 2\log(\det \mathbf{F})], \tag{2.13}$$

where N is the crosslink density in the reference state and $\mathbf{F} = F_{iK}$. kT is the temperature in the unit of energy; $k = 1.3806488 \times 10^{-23}\,\text{m}^2 \cdot \text{kg} \cdot \text{s}^{-2} \cdot \text{K}^{-1}$ the Boltzman constant; and T the absolute temperature.

In Eq. (2.12), there is both enthalpy and entropic contributions to the free energy density of mixing. We assume the Flory–Huggins form [Flory, 1942; Huggins, 1941]

$$W_{\text{mix}} = kT\left(C\log\left(\frac{\nu C}{1 + \nu C}\right) + \frac{\chi C}{1 + \nu C}\right), \tag{2.14}$$

where ν is the nominal volume of a solvent molecule and χ the interaction parameter.

In addition, the hydrogel is a condensed matter which we assume cannot be compressed, thus we express the condition of molecular incompressibility as

$$1 + \nu C = \det(\mathbf{F}). \tag{2.15}$$

Herein, the basic formulas of theory have been given. In Sec. 3, the theory can be applied to different types of hydrogels.

2.3. *Basic constitutive models for hyperelastic materials*

As most soft materials are simply regarded as hyperelastic materials, in this section, we first introduce the most common constitutive models for hyperelastic materials. Both the constitutive models of hydrogels and SMPs are based on these common constitutive models. One of the most common and simplest models is the Neo-Hookean model, whose strain-energy function can be expressed as follows:

$$W = \frac{1}{2}NkT(I_1 - 3), \tag{2.16}$$

where I_1 the first strain invariant, $I_1 = \lambda_1 + \lambda_2 + \lambda_3$, with λ_1, λ_2, λ_3 being the three principle stretches.

It should be noted that all the hydrogel models introduced in Sec. 3 are based on the Neo-Hookean model. However, other constitutive models for hyperelastic materials can also be developed into the constitutive models for hydrogels and SMPs. For example, Zhao *et al.* [2019] developed a model for large deformation and damage of interpenetrating polymer networks based on the Arruda–Boyce model, which is based on the statistical mechanics of a material with a cubic representative volume element containing eight chains along the diagonal directions. The strain

energy density function for the incompressible Arruda–Boyce model is given by [Boyce and Arruda, 2000]

$$W = NkT\sqrt{n}\left[\beta\lambda_{\text{chain}} - \sqrt{n}\ln\left(\frac{\sinh\beta}{\beta}\right)\right], \tag{2.17}$$

where n is the number of chain segments. β and λ_{chain} are relevant to the first invariant of the left Cauchy-Green deformation tensor $\mathbf{B} = \mathbf{F}\mathbf{F}^{\text{T}}$ [Boyce and Arruda, 2000]. Furthermore, the Gent model are used to build a hydrogel model that can describe the limiting chain extensibility [Okumura and Chester, 2018]. The strain energy density function for the Gent model is

$$W = -\frac{GJ_m}{2}\ln\left(1 - \frac{I_1 - 3}{J_m}\right), \tag{2.18}$$

where G is the shear modulus and $J_m = I_m - 3$. I_m is a limiting value of the first invariant. In the limit where $I_m \to \infty$, the Gent model reduces to the Neo-Hookean model.

These material models also apply to SMPs when considering the rubbery state at high temperature. For example, Diani *et al.* [2006] introduced a neo-Hookean law to express the entropy change η_0 from the free energy for shape memory polymers as follows:

$$-\eta_0 T = \frac{E^r}{6}\frac{T}{T_h}(I_1 - 3), \tag{2.19}$$

where E^r is the Young's modulus at the given temperature T_h, which represents the temperature above the range of the glass transition, and the polymer is considered to express rubber elasticity at this region.

There are also other available constitutive models for hyperelastic materials that can be used to develop future constitutive models of hydrogels and SMPs [Xiang *et al.*, 2018; Xiao *et al.*, 2019; Zhong *et al.*, 2019]. For example, there are the Mooney–Rivlin model, the Ogden model, and so on. In order to for further study of different constitutive models of soft materials, these widely adopted basic models will be introduced here as well. The strain energy density function for an incompressible Mooney–Rivlin material is

$$W = C_1(I_1 - 3) + C_2(I_2 - 3), \tag{2.20}$$

where C_1 and C_2 are empirically determined material constants, and I_2 is the second invariant which is defined as: $I_2 = \lambda_1\lambda_2 + \lambda_1\lambda_3 + \lambda_2\lambda_3$.

In the Ogden material model, the strain energy density is expressed in terms of the principal stretches λ_j, $j = 1, 2, 3$ as follows:

$$W(\lambda_1, \lambda_2, \lambda_3) = \sum_{p=1}^{L}\frac{\mu_p}{\alpha_p}(\lambda_1^{\alpha_p} + \lambda_2^{\alpha_p} + \lambda_3^{\alpha_p} - 3), \tag{2.21}$$

where L, μ_p and α_p are material constants.

These models are recommended for use in future studies to describe the mechanical behavior of hydrogels and SMPs.

2.4. *Basic viscoelasticity concepts*

In order to understand the constitutive models of hydrogel and SMPs, some basic concepts should be introduced first.

As mentioned earlier, the constitutive models of SMPs are mainly based on the viscoelastic theory of polymers. When subjected to external loadings, the polymers present a changing property between elastic solid and viscous liquid, termed viscoelasticity. For viscoelasticity, a dashpot element is a typical mechanical model to describe the viscosity when considering the viscous liquid. This model can be expressed as a piston in the cylinder which is full of Newtonian fluid. The basic formula is expressed as follows:

$$\sigma = \eta \frac{d\varepsilon}{dt}, \tag{2.22}$$

where η is the viscosity of the Newtonian fluid, and the strain ε in this model will be affected by the loading time and is considered as a rate-dependent property.

In order to present both the elasticity and viscosity, combined models with spring and dashpot elements have been introduced, and the most famous models would be Maxwell model and Kelvin model. Maxwell model integrates a spring and a dashpot in series to express the general mechanical performance of the viscoelastic polymer. The basic constitutive equation of a Maxwell model can be expressed as follows:

$$\frac{d\varepsilon}{dt} = \frac{1}{E}\frac{d\sigma}{dt} + \frac{\sigma}{\eta}, \tag{2.23}$$

where η and E satisfy the correlation $\eta = \tau E$, the scalar factor τ was defined as the relaxation time (retardation time) of the model. Similarly, the Kelvin model, which combines a spring and a dashpot in parallel, could also characterize the general performance of a viscoelastic material. On the basis of these viscoelastic models, researchers made several modifications to devise constitutive models of SMPs, such as introducing new elements and making different arrangements. The detail work will be present in Sec. 4.

To determine the parameters of SMP constitutive models, the concept of time temperature superposition principle is often used.

From the viscoelasticity theories, we already know that some mechanical properties of polymers will be affected by time. However, for SMPs, the temperature dependence on the mechanical parameters also needs be considered. With temperature increase, the glassy state of SMPs will transform into a soft rubbery state. Therefore, the correlations between mechanical parameters and temperature, as well as time must be coupled in the constitutive models. Following detailed experimental observations, researchers found an interesting phenomenon whereby relaxation curve at a certain temperature could be obtained by shifting the relaxation curve at various temperature regions within a fixed period of time. In other words, a same mechanical relaxation phenomenon could be observed either in a short time at high temperature or in a long time at low temperature. This is also defined as the time temperature superposition principle.

For thermo-rheological type materials, the shift factor usually follows the same rule which is commonly defined by empirical equations. The effect of changing temperature is simply to horizontally shift the viscoelastic response as a function of frequency. Therefore, the shift factor could be defined as the ratio of the relaxation time $\tau(T)$ and the reference relaxation time $\tau(T_r)$

$$a(T) = \frac{\tau(T)}{\tau(T_r)}. \tag{2.24}$$

To determine the shift factor $a(T)$, an empirical WLF equation [Di Marzio and Yang, 1997] was proposed accordingly

$$\log(a(T)) = \frac{-c_1(T - T_r)}{c_2 + (T - T_r)}, \tag{2.25}$$

where c_1 and c_2 are material constants that depend on the reference temperature T_r, and usually determined by fitting the experiment data.

3. Constitutive Models of Hydrogels

The basic formulas can be extended to different forms of constitutive models based on the different types of hydrogels. In this section, the constitutive models of six different types of hydrogels are presented, namely for neutral gel, salt concentration-sensitive gel, pH-sensitive gel, temperature-sensitive gel, photo-thermal sensitive gel, and magnetic sensitive gel.

3.1. *Constitutive model of neutral gel*

In the study of hydrogels, the neutral gel, whose only stimuli is the external exposure to water, is the most frequently studied type of gel. Thus, the neutral gel model, being the most basic type of hydrogel, has been studied extensively by many research groups. As there is no other stimulus, the constitutive model is based on the basic formulas mentioned in Sec. 2.

The free energy due to stretching a network of polymers is taken to be [Hong *et al.*, 2009]

$$W_{\text{str}} = \frac{1}{2}NkT(\lambda_1^2 + \lambda_2^2 + \lambda_3^2 - 3 - 2\log\lambda_1\lambda_2\lambda_3). \tag{3.1}$$

Let s_1, s_2 and s_3 be the three principal nominal stresses. Equation (2.11) is specialized to

$$s_1 = NkT(\lambda_1 - \lambda_1^{-1}) - \Pi\lambda_2\lambda_3, \tag{3.2}$$

and

$$s_2 = NkT(\lambda_2 - \lambda_2^{-1}) - \Pi\lambda_1\lambda_3, \quad s_3 = NkT(\lambda_3 - \lambda_3^{-1}) - \Pi\lambda_1\lambda_2, \tag{3.3}$$

$$\mu = kT\left[\log\frac{\nu C}{1+\nu C} + \frac{1}{1+\nu C} + \frac{\chi}{(1+\nu C)^2}\right] + \Pi\nu. \tag{3.4}$$

The general form of constitutive equations can be expressed as follows:

$$\frac{s_{iK}}{kT/v} = Nv(F_{iK} - H_{iK}) + \left[J\log\left(1 - \frac{1}{J}\right) + 1 + \frac{\chi}{J} - \frac{\mu}{kT}J\right]H_{iK}, \qquad (3.5)$$

where s_{iK} is the component of nominal stress.

Equations (3.2)–(3.5) constitute the equations of state for the neutral gel. The model can be used to describe the mechanical behaviors of the neutral gel such as the free swelling case, the deformation under uniaxial tension, etc. [Hong *et al.*, 2009].

3.2. *Constitutive model of salt concentration-sensitive gel*

When placed in an ionic solution, a network of polyelectrolytes imbibes the solution and swells, resulting in a salt concentration-sensitive gel. Like the neutral gel, the salt concentration-sensitive gel is subjected to geometric constraints and mechanical loads, but it is also under the stimulus of salt concentration, as illustrated in Fig. 4. The equilibrium of the chemical potential inside and outside of the gel provides thermodynamic equilibrium. One also defines the nominal concentration C_a as [Zheng and Liu, 2019]

$$C^a = c^a J, \qquad (3.6)$$

where $J = \det(\mathbf{F})$.

It should be noted that the nominal concentration C^a has been assumed as independent of J in many studies [Hong *et al.*, 2008, 2009; Liu *et al.*, 2010; Marcombe *et al.*, 2010]. For neutral gels [Hong *et al.*, 2008, 2009], the assumption is correct because the only concentration in the theory is that of the solvent. However, for the salt concentration-sensitive hydrogel [Liu *et al.*, 2010; Marcombe *et al.*, 2010],
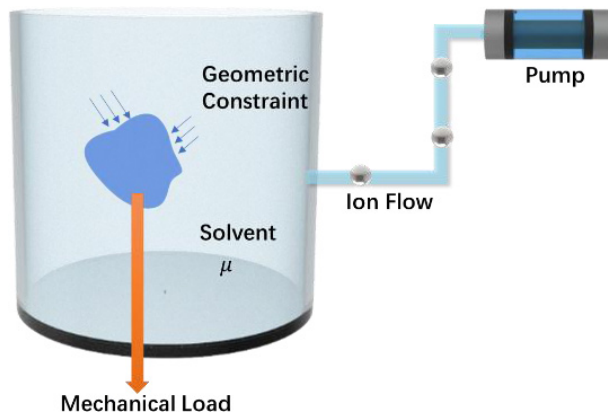

Fig. 4. A gel is in contact with a solvent with a fixed salt concentration and is subject to a mechanical load and geometric constraint, while ions flow from external sources into the gel through a field of pumps.

owing to the restriction of the Donnan equilibrium, C^a is related to J. Therefore, the original assumption is clearly erroneous based on the previous analysis [Zheng and Liu, 2019].

Besides the free energy density of stretching and mixing, the salt concentration-sensitive hydrogel also involves the free energy density due to the ions. Based on the free energy density function in Sec. 2, we further extend this approach by adding a term due to the ions

$$W = W_{\text{str}} + W_{\text{mix}} + W_{\text{ion}}, \tag{3.7}$$

where W_{ion} is the free-energy density of mixing the solvent and ions.

The free-energy density function of mixing the solvent and ions, which differs from that of the neutral gel, is assumed to be [Marcombe *et al.*, 2010]

$$W_{\text{ion}} = kT \left[C^+ \left(\log \frac{C^+}{c_{\text{ref}}^+ J} - 1 \right) + C^- \left(\log \frac{C^-}{c_{\text{ref}}^- J} - 1 \right) \right], \tag{3.8}$$

where c_{ref}^a is a reference value of the concentration of species a; here, we take c_{ref}^a to be c_0, the concentration in the salt solution. The unit of C^a is $[\text{m}^{-3}]$, rendering vC^a a dimensionless parameter.

To specify the relationship between the true concentration c^a and J, we introduce the well-known Donnan equations [Marcombe *et al.*, 2010]:

$$\frac{c^+}{c_0} = \frac{c_0}{c^-}, \tag{3.9}$$

where c_0 is the true concentration of the salt solution.

Furthermore, electroneutrality requires that [Liu *et al.*, 2010]

$$C_0 + C^- = C^+, \tag{3.10}$$

where C_0 is the fixed charges in the gel.

A combination of Eqs. (3.6), (3.9) and (3.10) yields

$$\frac{C_0}{J} + c^- = c^+. \tag{3.11}$$

With Eqs. (3.9) and (3.11), we obtain

$$c^+ = \frac{C_0}{2J} + \frac{1}{2} \sqrt{\frac{C_0^2}{J^2} + 4c_0^2}, \tag{3.12}$$

$$c^- = -\frac{C_0}{2J} + \frac{1}{2} \sqrt{\frac{C_0^2}{J^2} + 4c_0^2}. \tag{3.13}$$

Through the Donnan equation, the function W has been reduced to be dependent on only two independent variables $W(J, c_0)$. Furthermore, with the condition of molecular incompressibility enforced as a constraint, the theory specifies the true stress as

$$\sigma_{ij} = \frac{F_{jK}}{J} \frac{\partial W}{\partial F_{iK}} - \frac{\mu}{v} \delta_{ij}, \tag{3.14}$$

where μ is the chemical potential in the salt solution and can be specified as

$$\mu = -2kTvc_0. \tag{3.15}$$

From Eqs. (2.12) and (2.13), we obtain

$$\frac{\partial c^+}{\partial J} = -\frac{C_0}{2J^2} - \frac{1}{2}\frac{C_0^2}{J^3}\frac{1}{\sqrt{\frac{C_0^2}{J^2} + 4c_0^2}}, \tag{3.16}$$

$$\frac{\partial c^-}{\partial J} = \frac{C_0}{2J^2} - \frac{1}{2}\frac{C_0^2}{J^3}\frac{1}{\sqrt{\frac{C_0^2}{J^2} + 4c_0^2}}. \tag{3.17}$$

Using the function $W(J, c_0)$ and Eqs. (3.12)–(3.17), we obtain

$$\frac{\sigma_{ij}}{\frac{kT}{v}} = \frac{Nv}{J}(F_{iK}F_{jK} - \delta_{ij}) + \left(\log\frac{J-1}{J} + \frac{1}{J} + \frac{\chi}{J^2} + 2\nu c_0\right)\delta_{ij}$$

$$+ \nu\delta_{ij}\left[c^+\left(\log\frac{c^+}{c_0} - 1\right) + c^-\left(\log\frac{c^-}{c_0} - 1\right)\right.$$

$$\left. + J\left(\frac{\partial c^+}{\partial J}\log\frac{c^+}{c_0} + \frac{\partial c^-}{\partial J}\log\frac{c^-}{c_0}\right)\right]. \tag{3.18}$$

The model can describe the mechanical deformation of the salt concentration-sensitive gel, such as the free swelling case and the constrained swelling case. The model can also be implemented into the FEM code via ABAQUS subroutine [Zheng and Liu, 2019].

3.3. *Constitutive model of pH-sensitive gel*

The pH-sensitive hydrogel is a network of soft materials bearing acidic groups and in equilibrium with an aqueous solution and mechanical forces. Compared with the salt concentration-sensitive hydrogel, another free energy density part of dissociating the acidic groups can be added, resulting in the following free energy density function [Marcombe *et al.*, 2010]

$$W = W_{\mathrm{str}} + W_{\mathrm{mix}} + W_{\mathrm{ion}} + W_{\mathrm{dis}}, \tag{3.19}$$

where W_{dis} is due to dissociating the acidic groups.

It should be noted that due to the consideration of acidic groups, W_{ion} of a pH-sensitive gel is more complicated than that of a salt concentration-sensitive gel, namely,

$$W_{\mathrm{ion}} = kT\left[C^{H^+}\left(\log\frac{C^{H^+}}{c_{\mathrm{ref}}^{H^+}J} - 1\right) + C^+\left(\log\frac{C^+}{c_{\mathrm{ref}}^+J} - 1\right) + C^-\left(\log\frac{C^-}{c_{\mathrm{ref}}^-J} - 1\right)\right], \tag{3.20}$$

where C^{H+} is the nominal concentration of the hydrogen ion.

The free energy density part due to the dissociation of the acidic groups is taken to be

$$W_{\text{dis}} = kT \left[C^{A^-} \log\left(\frac{C^{A^-}}{C^{A^-} + C^{\text{AH}}} \right) + C^{\text{AH}} \log\left(\frac{C^{\text{AH}}}{C^{A^-} + C^{\text{AH}}} \right) \right] + \gamma C^{A^-},$$

(3.21)

where γ is the increase in the enthalpy when an acidic group dissociates; C^{A^-} and C^{AH} are the nominal concentration of the fixed charges and of associated acidic groups, respectively.

Using the function W specified above, Eq. (3.19) becomes

$$\frac{\sigma_{ij}}{\frac{kT}{v}} = \frac{Nv}{J}(F_{iK}F_{jK} - \delta_{ij}) + \left(\log\frac{J-1}{J} + \frac{1}{J} + \frac{\chi}{J^2} \right) \delta_{ij}$$

$$- v\delta_{ij}[c^{H^+} + c^+ + c^- - \bar{c}^{H^+} - \bar{c}^+ - \bar{c}^-],$$

(3.22)

where $\bar{c}^{H^+}$, $\bar{c}^+$, $\bar{c}^-$ are the concentration of the external solution.

It should be noted that the current study of the pH-sensitive hydrogel still assumes C^a to be independent of J and thus obtained Eq. (3.22). As stated in Sec. 3.2, the assumption is problematic as it cannot be properly implemented into the ABAQUS subroutine. Future studies can focus on a new model of pH-sensitive hydrogel which assumes C^a to be dependent of J.

3.4. *Constitutive model of temperature-sensitive gel*

Hydrogels that sustain huge volumetric change due to a change of temperature are called temperature sensitive hydrogels, which are also chemically known as PNIPAM hydrogels. These transparent, elastic and highly flexible hydrogels are an important branch of hydrogels due to their amazing property of having a sharp macromolecular transition from a hydrophilic to a hydrophobic structure at what is known as the lower critical solution temperature (LCST). When temperature is changed from below to above the critical temperature, the hydrogel undergoes a phase transition: the amount of water in the hydrogel in equilibrium changes with temperature discontinuously, as illustrated in Fig. 5.

The free energy density of the temperature sensitive hydrogel is the same as the neutral gel, consisting of the part of stretch and mixing. The difference, however, is the interaction parameter χ, which is determined experimentally, given in the form [Huggins, 1964]

$$\chi = \chi_0 + \chi_1\phi,$$

(3.23)

where $\chi_0 = A_0 + B_0T$, $\chi_1 = A_1 + B_1T$ and $\phi = \frac{1}{1+\nu C}$.

Here for the PNIPAM gel, we use the following fitting parameters [Afroze *et al.*, 2000]:

$$A_0 = -12.947, \quad B_0 = 0.04496\,\text{K}^{-1}, \quad A_1 = 17.92, \quad B_1 = -0.0569\,\text{K}^{-1}.$$
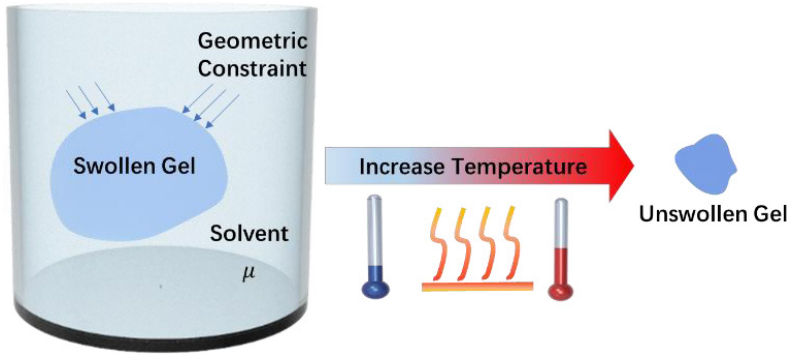
(3.24)

Fig. 5.   Schematic illustration of the swollen state to the collapsed state of temperature sensitive hydrogel.

We can also adopt the differential equation to obtain nominal stress. Here, for study purpose, we only consider a uniaxial load case. In this case

$$\lambda_1 = \lambda_2 = \sqrt{\frac{V}{V_0 \lambda_3}}, \tag{3.25}$$

where V is the volume of the gel and V_0 is the volume in the referential state.

Under uniaxial load, we obtain

$$\frac{\partial W(\lambda_1, \lambda_3, T)}{\partial \lambda_1} = 0, \tag{3.26}$$

$$\frac{\partial W(\lambda_1, \lambda_3, T)}{\partial \lambda_3} = s, \tag{3.27}$$

where s is the stress due to the uniaxial load.

Combining Eqs. (3.2)–(3.5), (3.26) and (3.27) we arrive at

$$N\nu(\lambda_1^2 - 1) + \left(\frac{V}{V_0}\right) \log\left[1 - \left(\frac{V}{V_0}\right)^{-1}\right]$$

$$+ 1 + (\chi_0 - \chi_1)\left(\frac{V}{V_0}\right)^{-1} + 2\chi_1\left(\frac{V}{V_0}\right)^{-2} = 0, \tag{3.28}$$

$$\frac{1}{\lambda_3}\left[N\nu(\lambda_3^2 - 1) + \left(\frac{V}{V_0}\right) \log\left[1 - \left(\frac{V}{V_0}\right)^{-1}\right]\right.$$

$$\left. + 1 + (\chi_0 - \chi_1)\left(\frac{V}{V_0}\right)^{-1} + 2\chi_1\left(\frac{V}{V_0}\right)^{-2}\right] = \frac{s\nu}{kT}. \tag{3.29}$$

It should be noted that one peculiar phenomenon of the temperature-sensitive hydrogel that aforementioned gels do not possess is the phase transition. For example, in the uniaxial load case, one stress may consist of two stretches, representing the phase transition process.
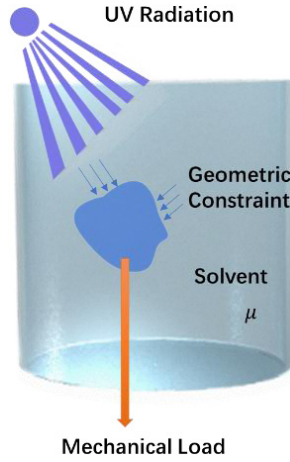
Fig. 6.   A hydrogel domain subjected to external weight P, exposed to an external solvent of fixed chemical potential μ, and irradiated with light.

3.5. *Constitutive model of photo-thermal sensitive gel*

The photo-thermal sensitive gel is a type of temperature sensitive hydrogel impregnated with light-absorbing nanoparticles as illustrated in Fig. 6. For a photo-thermal sensitive gel, an additional free energy density term due to photochemical reactions W_p is introduced into the free energy density function of a temperature sensitive hydrogel, namely [Toh *et al.*, 2014a],

$$W = W_{\mathrm{str}} + W_{\mathrm{mix}} + W_p, \tag{3.30}$$

where W_p is the free energy of photochemical reaction.

The free energy density W_p, resulting from photochemical reactions is expressed as

$$W_p = C_p\left[hf + kT \log\left(\frac{C_p}{C_{g,0}}\right)\right], \tag{3.31}$$

where hf corresponds to energy transition of the electron into the excited state and the logarithmic term corresponds to the entropy changes associated with the transition; C_p and $C_{g,0}$ are taken to be a nominal reference value given that the concentration of excited particles is low ($C_p/C_g \sim 10^{-10}$).

C_p can be expressed in terms of swelling ratio and light intensity

$$C_p = \left[\frac{c^{(w)}}{J} + \frac{c^{(\mathrm{network})} - c^{(w)}}{J^2}\right]\frac{\alpha I_0}{hf}, \tag{3.32}$$

where $c^{(w)}$ and $c^{(\mathrm{network})}$ are the volumetric heat capacities of water and the network, respectively; α is the proportionality constant related to the heat capacity of the gel; I_0 is the light intensity.

Using the function W specified above, Eq. (3.14) becomes

$$\frac{\sigma_{ij}}{\frac{kT}{v}} = \frac{Nv}{J}(F_{iK}F_{jK} - \delta_{ij}) + \left(\log\frac{J-1}{J} + \frac{1}{J} + \frac{\chi_0 - \chi_1}{J^2} + \frac{\chi_1}{J^3}\right)\delta_{ij}$$

$$+ v\frac{\alpha I_0}{hf}\left[\frac{2(c^{(\text{network})} - c^{(w)})}{J^3} + \frac{c^{(w)}}{J^2}\right]\delta_{ij} - \frac{\mu}{kT}\delta_{ij}. \tag{3.33}$$

The developed model of the photo-thermal sensitive gel can accurately and efficiently predict the deformation of photo-thermal sensitive gels with complex geometries.

3.6. *Constitutive model of magnetic-sensitive gel*

The incorporation of magnetic nanoparticles, such as super paramagnetic iron oxide nanoparticles (SPION) has caught the attention of materials scientists recently for its ability to undergo large deformation under remote control [Hu *et al.*, 2018a; Zhao *et al.*, 2019]. It should be noted that an alternative approach using multiphysics model to simulate the responsive behavior of the magnetic-sensitive hydrogel has also been carried out [Liu *et al.*, 2017].

Referring to Fig. 7, a gel is subjected to geometrical constraints and attached to a body force P_i and traction T_i and is maintained at chemical potential μ. Nearby, a wire of alternating current I, induces a magnetic field B in the gel. The work done on the gel by the mechanical load, solvent and magnetic field are $P\delta l$, $\mu\delta N$ and $B\delta M$, respectively.

Based on the free energy density function in Sec. 2, we further extend this approach by adding a term due to the magnetization:

$$W = W_{\text{str}}(F_{iK}) + W_{\text{mix}}(C) + W_{\text{mag}}(M). \tag{3.34}$$
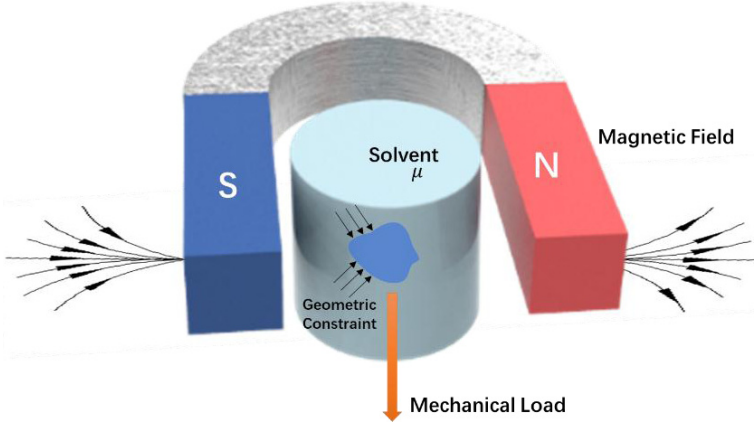

Fig. 7. External loads on a magnetic gel that under magnetic field.

We assume the simplest case of a paramagnetic system with spin $\frac{1}{2}$ ground state and no orbital angular momentum. Under this assumption,

$$W_{\text{mag}} = -N_m kT \left\{ \ln \left[2 \cosh \left(\frac{\mu_B B}{kT} \right) \right] \right\}, \tag{3.35}$$

where N_m is the number of magnetic particles per unit reference volume, μ_B is the chemical potential of the magnetic gel.

In a gel with SPIONs, the magnetization is proportional to the magnetic particle concentration and takes the form of a hyperbolic tangent function [Stöhr and Siegmann, 2006], i.e.,

$$M = \phi_m N_m \mu_B \tanh \left(\frac{\mu_B B}{kT} \right). \tag{3.36}$$

Given that ϕ_m the concentration of magnetic particles within the polymer network does not change with swelling, we can write $f_m + f_p = 1$, where f_m is the volume fraction of magnetic particles with the polymer network and can be regarded as a material parameter.

Combining with Eq. (3.36), we find that the magnetization is inversely proportional to the volume swelling ratio, J

$$M = \frac{f_m N_m \mu_B}{J} \tanh \left(\frac{\mu_B B}{kT} \right). \tag{3.37}$$

We obtain the values of N_m by equating temperature rise during magnetic hyperthermia to the total energy of all magnetic dipoles during the magnetization process

$$N_m \mu_B B \tanh \left(\frac{\mu_B B}{kT} \right) = \rho c \Delta\theta, \tag{3.38}$$

where $\Delta\theta$ is the temperature difference, and for SPIONs gel, $\rho = 1480 \, \text{kg m}^{-3}$ and $c \approx 2230 \, \text{Jk g}^{-1} \, \text{K}^{-1}$. The nominal stress is thus

$$\frac{s_{ik}\nu}{kT_0} = N\nu \frac{T}{T_0}(F_{iK} - H_{iK}) + \frac{T}{T_0} \left[\ln \left(\frac{J-1}{J} \right) + \frac{1}{J} + \frac{\chi_0 - \chi_1}{J^2} + \frac{2\chi_1}{J^3} \right] J H_{iK}$$

$$- \bar{\mu}^s J H_{iK} + N_m \nu f_m \frac{\bar{B} \tanh(\bar{B}\frac{T_0}{T})}{J^2} J H_{iK}, \tag{3.39}$$

where $F_{iK} H_{jK} = \delta_{ij}$ and $\overline{B} = \frac{\mu^s B_{\text{mag}}}{k_B T}$ is the dimensionless strength of the magnetic field.

Above we discussed the constitutive models of hydrogels. The developed models can accurately and efficiently predict the deformation of different types of gels with complex geometries. Likewise, in Sec. 4, we will introduce the constitutive models of SMPs.

4. Constitutive Models of Shape Memory Polymers

As a fast-emerging type of smart material, SMPs have been rapidly applied in many different industrial areas in the past few decades and also attracted huge research interests. To investigate the mechanical behavior and the underlying mechanisms of SMPs structures, it is imperative to propose suitable and robust constitutive models for describing the shape memory effect in a detailed manner. Compared with other shape memory materials, SMPs can be triggered by different stimuli such as light, electricity, water/moisture, magnetism, etc. Although different types of SMPs require distinct consideration for each unique external stimulus effect, the intrinsic mechanisms of the SMPs deformation all follow similar considerations with thermal-induced SMPs. Therefore, thermal-induced SMPs dominate most of the research efforts in the theoretical studies of SMP materials. There are many different approaches towards thermal-induced SMPs to consider and examine the mechanisms and principles of shape memory phenomenon such as stress-strain relationships under various conditions and the dependence on temperature, time, strain-rate or other factors. Generally, the constitutive models of thermal-induced shape memory polymers can be divided into the following two categories: firstly the rheological models based on the viscoelastic theory with rate/temperature-dependent property parameters; secondly the micromechanical phenomenological models based on the concept of phase transition. Consequently, we will discuss the constitutive models of SMPs from these two perspectives in Secs. 4.1–4.3.

4.1. *Rheological models of shape memory polymer*

The rheological model with temperature-dependent viscosity and modulus parameters is a very important approach for thermal-induced SMPs. Several springs and dashpot elements are adopted in this type of model. Since the model parameters vary on temperature, these models can quantitively describe the shape memory effects of SMPs. These models can also accurately characterize the viscoelastic behaviors of SMPs, such as creep and stress relaxation. Besides, it can effectively evaluate mechanical properties dependent on temperature, time, strain rate and other factors as well.

4.1.1. *Basic viscoelastic model*

The earlier researchers mainly adopted the linear viscoelastic models and made proper modifications to describe the thermomechanical behaviors of the SMPs. Based on a parallel combination of the spring-dashpot elements and a slip unit, Tobushi *et al.* [1997] first proposed a rheological 4-element model which can describe the thermo-viscoelastic behavior of SMP undergoing small 1D deformation. Referring to Fig. 8, a standard linear viscoelastic model including the spring-dashpot elements is applied to characterize the linear viscoelasticity and the overall mechanical behaviors of SMPs.
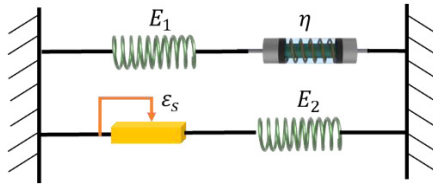
Fig. 8.   The basic four-element model of SMPs.

Meanwhile, the slip mechanism due to internal friction is introduced to express the creep recovery strain above and below the glass transition temperature region. In addition to the representation of the general viscoelasticity with such elements, heat expansion due to temperature change of a complete thermal cycle has also been considered in this constitutive model. For this model, the stress-strain relationship is expressed as follows:

$$\dot{\varepsilon} = \frac{\dot{\sigma}}{E} + \frac{\sigma}{\eta} - \frac{\varepsilon - \varepsilon_s}{\tau} + \alpha \dot{T}, \tag{4.1}$$

$$\varepsilon_s = c(\varepsilon_c - \varepsilon_l), \tag{4.2}$$

where σ, ε and T denote the stress, strain and temperature, respectively. The key material parameters E, η, τ and α are the elastic modulus, viscosity, relaxation time and heat expansion coefficient, respectively, while ε_c and ε_l denote the creep strain and its critical value. Besides, based on the observation of creep tests of SMPs, the irrecoverable creep strain ε_s due to slip (when force larger than internal friction) is assumed to be in a proportional relationship with the creep strain.

To calibrate the parameters of the proposed constitutive model, Tobushi *et al.* [1996a,b] carried out a series of experimental tests for SMPs of the polyurethane series. The experiments demonstrated distinctive mechanical performance but revealed a general law of SMPs. The mechanical properties of SMPs in the glass transition region vary significantly, and the material coefficients are highly dependent on the temperature. Based on the dynamic mechanical test results, the elastic modulus E can be expressed by a single exponential function of temperature as

$$E = E_g \exp\left\{ a_E \left(\frac{T_g}{T} - 1 \right) \right\}, \tag{4.3}$$

where T_g represents the glass transition temperature. E_g denotes Young's modulus value when $T = T_g$, and a_E is the slope of the straight line through fitting of the experiment data. Similarly, the variation curves of other mechanical coefficients such as η, τ, c and ε_l (viscosity, relaxation time, heat expansion coefficient and creep strain) due to the glass transition will basically coincide with those of E. Therefore, to express the deformation performance of SMPs at the glass transition region, all material parameters can be expressed in the same manner as

$$G = G_g \exp\left\{ a_G \left(\frac{T_g}{T} - 1 \right) \right\}. \tag{4.4}$$

Here, the material parameters E, τ, λ, c and ε_l are all accounted for by G and expressed as the exponential functions of temperature. G_g is the value of distinctive G when the temperature is in the glass transition region, and a_G denotes the corresponding slope of each straight line as observed in experimental data.

The above constitutive model has been proven to provide very good agreement with the thermomechanical behaviors observed from the experiments for some SMPs. This linear constitutive model provides a simple method to effectively predict the material properties such as shape fixity, shape recovery and recovery stress. However, the validity of this simple model applied to small 1D deformation cases, namely the model expressed well with the thermomechanical properties only up to 10% of strain. To express the material properties of SMPs for relatively large deformation from the practical viewpoint, Tobushi *et al.* [2001] introduced nonlinear terms of stress as an exponential function for both the elastic term and the viscous term into the framework of the earlier linear constitutive equations. The detailed stress-strain relationship can be expressed as follows:

$$\dot{\varepsilon} = \frac{\dot{\sigma}}{E} + m\left(\frac{\sigma - \sigma_y}{k}\right)^{m-1}\frac{\dot{\sigma}}{K} + \frac{\sigma}{\eta} + \frac{1}{b}\left(\frac{\sigma}{\sigma_c} - 1\right)^n - \frac{\varepsilon - \varepsilon_s}{\tau} + \alpha\dot{T}, \quad (4.5)$$

$$\varepsilon_s = S(\varepsilon_c + \varepsilon_p). \tag{4.6}$$

This new constitutive model adds nonlinear terms of stress as a power function to the previous linear model framework, σ_y and σ_c correspond to the yield stress and creep limit, respectively. Defined in the same manner as the linear model, the irrecoverable creep strain ε_s is assumed to be proportional to the creep strain at a ratio S. However, a remaining plastic strain denoted by ε_p at the recovery stage which corresponds to the large predeformation must also be considered in the model. Similar to Eq. (4.1), material parameters $E, k, \sigma_y, \mu, \sigma_c, \tau$ and S involved in this model would be accounted for by a single exponential function of temperature. Other material parameters including m, n, b and α have weak dependence on temperature and are therefore assumed to be temperature independent for simplicity. In general, the proposed nonlinear model is applied to calculate several results of different thermomechanical tests and could well express the general properties of the SMPs in the strain range of practical use (up to 20% maximum strain). Besides, this model could effectively characterize the working performance of the SMPs such as the working temperatures, the shape memory effect, the tightening force and the response speed, which could be helpful in the design of SMP elements. Tobushi *et al.*'s models are based on the basic spring-dashpot elements framework. Similarly, Morshedian *et al.* [2005] combined Kelvin unit and a dashpot element in series to establish a mechanical model to describe the stress-strain-time relationship of the crosslinked PE SMP.

Inspired by the same framework, Li *et al.* [2015] proposed a simplified three-element model and effectively simulated the stress-strain-temperature characteristics of polyurethane-SMP for both free and constrained strain recovery process. This

model combined a standard Kelvin element and a spring element in series, therefore an overall 3-elements (2 springs and 1 dashpot) model framework was established. The 1D constitutive equations of this model can easily be derived as:

$$\sigma + \frac{\mu(T)}{(E_1(T) + E_2(T))}\frac{d\sigma}{dt} = \frac{\mu(T)}{(1 + E_1(T)/E_2(T))}\left(\frac{d\varepsilon}{dt} - \alpha\frac{dT}{dt}\right)$$
$$+ \frac{1}{(1/E_1(T) + 1/E_2(T))}(\varepsilon - \alpha(T - T_0)). \quad (4.7)$$

This constitutive model was then applied to develop a UMAT subroutine in ABAQUS and was generalized to a 3D isotropic solid form to simulate the shape memory behaviors of SMPs. It should be noted that glass transition temperature T_g, the coefficient of thermal expansion $\alpha(1/K)$, and elastic modulus $E(T_g)$, retardation time $\tau(T_g)$, viscosity $\eta(T_g)$ were determined based on earlier obtained experimental data [Tobushi *et al.*, 1997]. Compared with the experimental data, this model provides a better prediction for both free and constrained shape recovery process. In short, this model can efficiently predict SMP response with just simplified modal parameters, which is very useful for some engineering applications.

These early thermo-constitutive models adopted the simple dashpot and spring elements and by different arrangements of these units were able to represent the main features of the mechanical behaviors of the SMP materials. For some engineering applications, these simple and effective models offer much convenience for basic modelling and simulation purposes.

4.1.2. *Thermoviscoelastic models of SMPs coupled with temperature and rate effects*

Although previous models based on well-known standard linear viscoelastic elements provide a simple method to quantitively represent the general mechanical properties of the SMPs, these constitutive models mainly focused the infinitesimal strains. Based on the viscoelastic properties and the thermomechanical considerations of the SMPs, Diani *et al.* [2006] developed a 3D thermo-viscoelastic constitutive model to account for large strain deformation behaviors. During a typical thermomechanical loading cycle of the SMP, the deformation change is correlated with changes in entropy and internal energy. Based on thermodynamics, the Helmoholtz free energy of SMP is decomposed as:

$$W = U(\mathbf{F}^e) - \eta_0 T(\mathbf{F}), \quad (4.8)$$

where the entropy η_0 is dependent on the total deformation gradient $\mathbf{F}$, and the internal energy is simply a function of viscous deformation $\mathbf{F}^v$ (or equivalently $\mathbf{F}^e$). The free energy in this model is then applied in a neo-Hookean law as expressed in Eq. (2.16), and the Clausius–Duhem inequality is introduced as the thermodynamic requirements for the evolution of the overall deformation. As explained in Eq. (2.5), the deformation from the entropy and the internal energy are expressed in different

ways. Therefore, the total Cauchy stress due to changes in entropy and internal energy can be expressed accordingly as follows:

$$\left\{\begin{array}{ll} \boldsymbol{\sigma}^\eta = \dfrac{E^r}{6}\dfrac{T}{T_h}\mathbf{F}^e\mathbf{F}^{eT} - p\mathbf{I} & \text{(stress from entropy branch)} \\[2mm] \boldsymbol{\sigma}^U = \mathbf{L}^e[\ln(\mathbf{V}^e)] & \text{(stress from internal energy branch)} \end{array}\right\}, \quad (4.9)$$

where p is a Lagrange multiplier dependent on the boundary conditions, L^e the elastic constant tensor assumed to be temperature independent, and V^e the left stretch tensor decomposed from the deformation gradient $\mathbf{F}^e$, or equivalently $\mathbf{F}^v$. To compute $\boldsymbol{\sigma}^U$, one can use the evolution of $\mathbf{F}^v$ based on earlier observations and the mechanical dissipation in the form of the velocity gradient corresponding to $\mathbf{F}^v$ into the equations. All other material parameters including Young's modulus and thermal expansion coefficients can be estimated based on actual experimental testing for both above and below T_g. Generally, this model can accurately estimate the remaining strain during stress release and provide a useful framework to predict the thermomechanical response of SMPs undergoing large deformation.

Previous rheological models mainly discussed the mechanical performance of SMPs with temperature dependence. Later on, researchers began to investigate both temperature and rate effect on polymer viscosity (stress relaxation, creep retardation time, loading rate, etc.). Buckley *et al.* [2007] introduced the Kohlrauche Williams Watts equation for rubbery material (an empirical formula of creep curve) into the thermo-viscoelastic models of shape memory material and successfully described the polymer's temperature dependence on the retardation time. This approach could be applied to predict the shape recovery during the heating recovery process by first measuring their thermoviscoelastic response in the linear viscoelastic region. Subsequently, Nguyen *et al.* [2008] found that structure relaxation in the glass transition region (below T_g) and stress relaxation within the whole temperature range are two important factors that determined the rate-dependence of the shape memory response of amorphous SMPs. Structure relaxation mainly describes the rate dependence on the temperature and pressure while the stress relaxation focusses more on the rate dependence on the mechanical loading change. Based on a linear thermoviscoelastic rheological model, the nonlinear formulation of Adam-Gibbs model was introduced to characterize the temperature and rate dependence on structural relaxation. Meanwhile, a modified Eyring temperature-dependent flow rule was adopted in the model to simulate the stress relaxation response spanning the glass transition region. With consideration of a nonequilibrium process for both structural and stress relaxation, this model can provide good fits to the stress-free strain temperature response and strain-rate dependent stress-strain response for SMPs. Furthermore, a number of other groups attempted to investigate the thermal effect and rate effect on the SMPs based on their respective assumptions in a rheological base, the details of which will not be enumerated here [Castro *et al.*, 2010; Ghosh and Srinivasa, 2013; Zeng *et al.*, 2018].

4.1.3. *Fractional viscoelastic constitutive model*

Classical viscoelastic models such as the Generalized Maxwell model and Kevin model usually include differential operators of integer order, which provide exponential type relations between relaxation modulus and time. However, many types of SMPs are expressed by relaxation behavior of power-law type, which lead to a large number of material parameters to be determined from experiments. For Example, there are 31 material parameters in the previously discussed model of Diani *et al.* [2006]. Attempting to describe complex viscoelastic behavior with less parameters, Pan and Liu [2018] applied the fractional viscoelastic model to systematically investigate the thermomechanical behaviors of SMPs and conducted a series of thermomechanical experiments to verify the model parameters. The schematic of the proposed model is presented in Fig. 9. The mechanical branches combine two fractional Maxwell elements (nonequilibrium branches) and a Hookean spring (equilibrium branch) in parallel. The thermal expansion was considered independent of the mechanical behaviors and defined by

$$\varepsilon_T = \alpha(T - T_0). \tag{4.10}$$

Following the rule of fractional calculus, the fractional differential equation of each Maxwell element in this model can be given as

$$\frac{D^\beta \sigma_{\mathrm{FM}}}{Dt^\beta} + \frac{1}{\tau^\beta}\sigma_{\mathrm{FM}} = E\frac{D^\beta \varepsilon_{\mathrm{FM}}}{Dt^\beta}, \quad 0 < \beta < 1, \tag{4.11}$$

where E is the stiffness of the spring, τ the relaxation time and β is a decimal between zero and one. σ_{FM} and $\varepsilon_{\mathrm{FM}}$ are the stress and strain in a fractional Maxwell element, respectively.

The corresponding explicit stress-strain relationship can be derived by Laplace transformation as

$$\sigma_{\mathrm{FM}}(t) = E\int_{t_0}^t E_\beta\left(-\left(\frac{(t-\xi)}{\tau}\right)^\beta\right)\frac{d\varepsilon_{\mathrm{FM}}(\xi)}{d\xi}d\xi + E_\beta\left(-\left(\frac{t-t_0}{\tau}\right)^\beta\right)\sigma_{\mathrm{FM}}(t_0),$$

$$\tag{4.12}$$

$$E_\beta(x) = \sum_{n=0}^{\infty}\frac{x^n}{\Gamma(\beta n + 1)}, \tag{4.13}$$
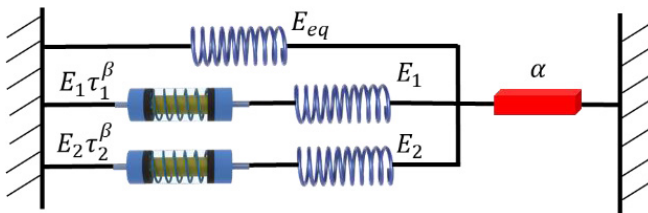

Fig. 9.   Schematic of generalized fractional viscoelastic model.

where E_β is the Mitting-Leffler function and n belongs to the set of integers. Finally, the total mechanical stress σ_M is derived by adding all branches in the model:

$$\sigma_M(t) = \sigma_{\text{eq}}(t) + \sum_{i=1}^{m} \sigma_i(t)$$

$$= E_{\text{eq}}\varepsilon_M(t) + \sum_{i=1}^{2}\left[E_i \int_{t_0}^{t} E_\beta\left(-\left(\frac{(t-\xi)}{\tau_i}\right)^{\beta}\right) \frac{d\varepsilon_M(\xi)}{d\xi}d\xi \right.$$

$$\left. + E_\beta\left(-\left(\frac{t-t_0}{\tau_i}\right)^{\beta}\right)\sigma_i(t_0) \right]. \tag{4.14}$$

Pan and Liu [2018] also conducted several thermomechanical experiments to verify the model parameters. By shifting the storage modulus-frequency curves measured in Fig. 10, the shift factors can be obtained.

As shown in Table 1, this proposed fractional constitutive model requires only 11 material parameters to be determined, which is a significant reduction compared with previous complex models. With lesser parameters, this model could capture the thermomechanical behaviors of SMPs with very good agreement with experimental results of shape memory free recovery
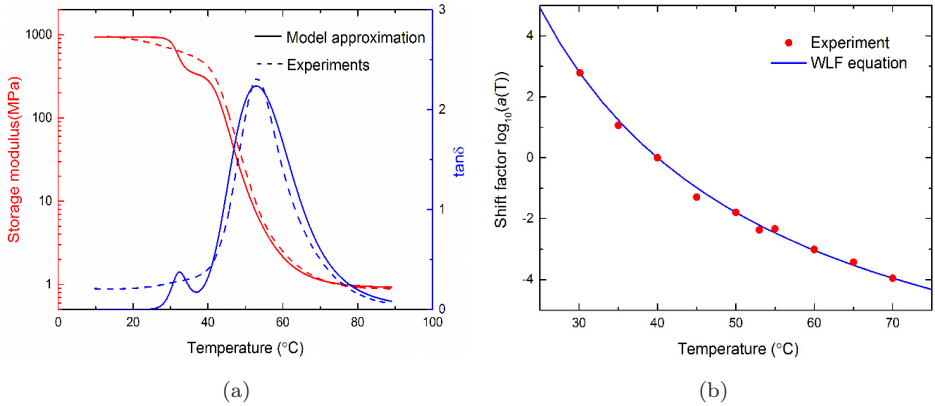

Fig. 10. (a) Storage modulus and tan δ master curves of the SMP obtained by horizontally shifting the frequency sweep tests at a reference temperature of 40°C and (b) WLF equation approximation of the shift factors.

Table 1.   Material parameters which need be determined.

Material parameters	E_{eq}	E_1	E_2	τ_1	τ_2	β	c_1	c_2	T_r	α_r	α_g
Values	0.9 Mpa	335.77 Mpa	596.56 Mpa	0.6065 s	0.0008 s	0.793	9.91	45.23°C	40°C	2.1e-4	3.2e-5

4.2. *Phenomenological models of shape memory polymer*

A typical phenomenological model for shape memory polymer is based on the
"meso-mechanical approach" which decomposed the SMPs to multiple continuous
structures ("phases"). Under certain external excitations such as temperature, the
different phases can transform each other and therefore reflect the corresponding
properties of the SMP. Generally, the deformation of the phase above glass transi-
tion temperature T_g was assumed "active" and the phase below T_g "frozen". These
phases are assumed to deform in parallel, and the rule of mixtures is applied as the
mechanical constraints to calculate the stress response from those of the individual
phases for SMPs. Compared with the rheological model of SMPs, the phenomeno-
logical model could effectively relate the phase transition concept with the shape
memory effect, so as to provide a clearer and more thorough understanding of the
deformation mechanism in SMPs.

4.2.1. *Classic phenomenological constitutive model*

The earliest phenomenological 3D model for T_g-activated SMPs was proposed by
Liu *et al.* [2006]. In this work, the SMP structure is considered as a mixture of
two phases: the frozen phase (dark shaded in Fig. 11) where the internal energic
change dominates the deformation and the high temperature entropic deformation
is completely locked; and the active phase (light shaded region in Fig. 11) where
the polymer free entropic conformation motion occurs.

The frozen phase is the major phase of a polymer in the glassy state while the
active phase mainly centers around the rubbery state. By changing the fraction of
the two phases, the large-scale conformation motion at high temperature can be
locked at the frozen phase and released once the temperature recovers. This mecha-
nism implies a complete deformation cycle of a SMP. Based on different phases, this
model decomposes the strain energy to thermal, elastic strain and frozen entropic
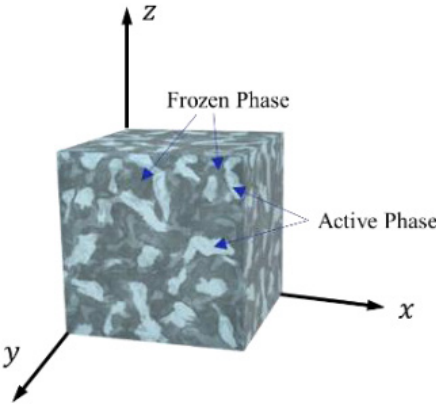

Fig. 11.   Schematic of the two phases mixture of SMPs.

(stored) strain components and applies the frozen volume fraction as internal variables to describe the microstructure evolution. For simplicity, the volume fraction is assumed to be only temperature dependent and the corresponding stress in two phases is equal even though the whole material of SMP is inhomogeneous. The total strain ε can be expressed as

$$\varepsilon = \left(\frac{1}{V} \int_0^{v_{\text{frz}}} \varepsilon_f^e(X) \mathrm{d}v \right) + (\phi_f \varepsilon_f^i + (1 - \phi_f) \varepsilon_a^e) + (\phi_f \varepsilon_f^T + (1 - \phi_f) \varepsilon_a^T), \quad (4.15)$$

where the subscripts f and a denote the frozen and active phases, respectively. The superscripts e, i and T corresponds to the average of the frozen (stored) entropic strain, the internal energetic strain, and the thermal strain, respectively. The frozen volume fraction ϕ_f is defined by the rules of mixtures. For simplicity, the total deformation is decomposed into three parts, refer to right-hand side of Eq. (4.15). The first part is the frozen entropic (stored) strain ε_s, and the second part is defined as a mechanical strain ε_m that follows the Generalized Hooke's law since the nonlinearity is neglected for small deformation. The third part is defined as the thermal strain ε_T and assumed to be dependent on the equivalent homogeneous thermal expansion coefficient.

From free strain recovery experiments, the frozen fraction ϕ_f can be found to be the strain ratio $\varepsilon^*/\varepsilon_{\text{pre}}$ if the thermal and internal energetic strain are neglected. The modified strain ε^* reflects the real strain stored in the frozen phase and ε_{pre} is defined as the pre-deformation strain in the preload process. Consequently, ϕ_f could be expressed as a phenomenological function of temperature, and the detail formula can be written as follows:

$$\phi_f = 1 - \frac{1}{1 + c_f (T_h - T)^n \frac{\varepsilon^*}{\varepsilon_{\text{pre}}}}, \quad (4.16)$$

where the two variables c_f and n are dependent on temperature and can be determined by fitting the strain ratio $\varepsilon^*/\varepsilon_{\text{pre}}$.

It should be noted that the change of ϕ_f here is dependent only on temperature while the rate effect (cooling/heating rate) is neglected. Besides, the Young's modulus E in this model has correlation with ϕ_f and the 1D form is given as

$$E = \frac{1}{\frac{\phi_f}{E_i} + \frac{1 - \phi_f}{E_e}}, \quad (4.17)$$

where E_i is the modulus corresponding to the glassy state at low temperature, and E_e the modulus corresponding to the entropic deformation at rubbery state. Also, E_i is considered as a temperature independent constant, while E_e is defined as the linear function of absolute temperature $E_e = 3NkT$.

Based on earlier definition, the overall constitutive equation for SMPs in a thermomechanical cycle in 1D form can be expressed as follows:

$$\boldsymbol{\sigma} = \frac{\varepsilon - \varepsilon_s - \varepsilon_T}{\frac{\phi_f}{E_i} + \frac{1 - \phi_f}{E_e}} = E \left(\varepsilon - \varepsilon_s - \int_{T_h}^T \alpha \mathrm{d}T \right). \quad (4.18)$$

Here, the coefficient of thermal expansion α is defined as $\frac{d\varepsilon_T}{dT}$, and parameters ϕ_f, E_i and E_e can all be derived from curve fitting and are considered only temperature dependent in this model. For example: for an epoxy resin, the following coefficient can be adopted: $\alpha = 1.42 \times 10^{-6}T - 3.16 \times 10^{-4}(1/K)$ $n = 4$, $c_f = 2.7610^{-5}(1/K^4)$, $N = 9.86 \times 10^{-4}(\text{mol/cm}^3)$, and $E_i = 813$ Mpa.

Overall, this work provides an essential framework of a phenomenological model for T_g-activated SMPs (here it mainly refers to an epoxy resin) without consideration of rate dependence and large deformation (beyond $\pm10\%$). Based on 1D experimental results, the frozen fraction function can be determined to illustrate the micromechanics and underlying physics of the glass transition and the shape memory effect. The proposed constitutive model can predict the uniaxial stress responses under various thermomechanical conditions with proper fitting parameters.

Based on the modeling of polymer crystallization, Barot and Rao [2006] developed a constitutive model for temporary-type CSMPs (crystallizable shape memory polymers). In the model, the temporary shape is fixed as a crystalline phase and recovers to its original shape by melting the crystalline phase. The proposed model can take into consideration the high-temperature rubbery phase, the semi-crystalline phase, the crystallization process as well as the melting process by employing the multiple natural configuration framework. Within this framework, both the amorphous and crystalline phases of the SMPs have the tendency to return to its natural configuration, which represent the basis of the shape-memory behavior in this approach. In this model, the general thermodynamic consideration is employed to validate the model and a rate equation for the melting process is prescribed to simplify the process. The model can be applied to qualitatively represent typical shape-memory cycles under both uniaxial deformation and circular shear, and it has been shown that the results from the constant strain case achieve very good agreement with experimental data.

4.2.2. *Phenomenological models of SMP considering rate effect*

Following the similar concept of the previous model [Liu *et al.*, 2006], Li *et al.* [2017b] proposed a new phase-evolution-based thermomechanical constitutive model to describe the shape memory behaviors of amorphous SMPs, and the detailed framework of the model is presented in Fig. 12.
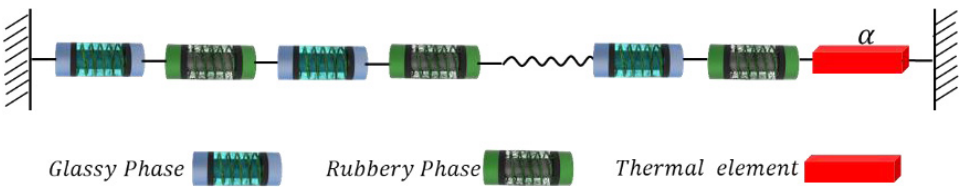

Fig. 12. Schematic representation of the proposed constitutive model.

The phase transition of material is a continuous process and can therefore be divided into small domains. Here, each rubbery phase has the volume fraction $\Delta\gamma_r^j$ and each glassy phase has the volume fraction $\Delta\gamma_g^j$, which corresponding to the ith rubbery phase and the jth glassy phase. The total volume fractions satisfy $\Sigma\Delta\gamma_g^j + \Sigma\Delta\gamma_r^j = 1$ and the total strain can be given as

$$\varepsilon_{\text{total}} = \Sigma\Delta\gamma_r^j\varepsilon_{\text{rubbery}}^j + \Sigma\Delta\gamma_g^j\varepsilon_{\text{glassy}}^j + \varepsilon_T, \tag{4.19}$$

where ε_T is the thermal strain, $\varepsilon_{\text{rubbery}}^j$ the strain in the jth rubbery phase domain with a volume fraction of $\Delta\gamma_r^j$, and $\varepsilon_{\text{glassy}}^j$ the strain the jth glassy phase domain with a volume fraction of $\Delta\gamma_g^j$. During a complete evolution cycle, the rubbery phase domain is assumed to undergo a mechanical deformation $F_{r-\text{mechanics}}$ at loading phase. During temperature reduction, the frozen deformation is locked in the glassy state and is denoted by F_{frozen}. The residual mechanical deformation in the glassy phase domain is denoted by $F_{g-\text{mechanics}}$. With the above analysis, the contributions of the mechanical strain and frozen strain to the total strain can be expressed as follows:

$$\varepsilon_{\text{total}} = \Sigma\Delta\gamma_r^j\varepsilon_{r-\text{mechanics}}^j + \Sigma\Delta\gamma_g^j(\varepsilon_{g-\text{mechanics}}^j + \varepsilon_{\text{frozen}}^j) + \varepsilon_T. \tag{4.20}$$

For simplicity, the volume fraction of glassy phase would be replaced by $\gamma = \Sigma\Delta\gamma_g^j$, then, the fraction of the rubbery phase can be obtained as $\Sigma\Delta\gamma_r^j = 1 - \gamma$. The total strain can be further generalized as

$$\varepsilon_{\text{total}} = \varepsilon_m + \varepsilon_f + \varepsilon_T, \tag{4.21}$$

where $\varepsilon_m = (1 - \gamma)\varepsilon_{r-\text{mechanics}} + \gamma\varepsilon_{g-\text{mechanics}}$ represents the total mechanical strain in the materials and $\varepsilon_f = \Sigma\Delta\gamma_g^j\varepsilon_{\text{frozen}}^j$ represents the total frozen strain in the materials.

Within these definitions, the author derived a series of equations to describe the mechanical behaviors during a complete thermal mechanical cycle. The constitutive equations of SMPs during cooling and heating process are summarized as follows:

$$\begin{cases} \sigma_{\text{total}} = \dfrac{\varepsilon_{\text{total}} - \varepsilon_f - \varepsilon_T}{\frac{\gamma}{E_g} + \frac{1-\gamma}{E_r}}, \\ \dfrac{d\varepsilon_f}{dT} = \dfrac{d\gamma}{dT}[1 - f(T)]\dfrac{\varepsilon_{\text{total}} - \varepsilon_f - \varepsilon_T}{E_r(\frac{\gamma}{E_g} + \frac{1-\gamma}{E_r})}. \end{cases} \tag{4.22}$$

Under the same boundary condition, the stress evolution paths during heating almost exactly overlay the stress-temperature curves during cooling, which is also in agreement with the experimental observations. Li *et al.* [2017a] provided a phase-evolution-based constitutive model which is quite similar to previous phenomenological models. However, the frozen strain in these models is considered to be only temperature dependent. In an actual situation, it takes time to freeze the strain. This model simplification may compromise the reliability of the method. Therefore, an improved constitutive equation was also discussed in Li *et al.*'s work

by introducing a time factor into the evolution of the frozen strain. By replacing the frozen strain with the real frozen strain $\varepsilon_{f-\text{real}}$, the updated new model can be expressed as follows:

$$\begin{cases} \sigma_{\text{total}} = \dfrac{\varepsilon_{\text{total}} - \varepsilon_{f-\text{real}} - \varepsilon_T}{\frac{\gamma}{E_g} + \frac{1-\gamma}{E_r}}, \\[2ex] \dfrac{d\varepsilon_f}{dT} = \dfrac{d\gamma}{dT}[1 - f(T)]\dfrac{\varepsilon_{\text{total}} - \varepsilon_f - \varepsilon_T}{E_r(\frac{\gamma}{E_g} + \frac{1-\gamma}{E_r})} \\[2ex] \varepsilon_{f-\text{real}} = \varepsilon_f - \displaystyle\int_0^t \dot{\varepsilon}_f e^{\frac{-(t-a)}{\tau}} da. \end{cases} \qquad (4.23)$$

To verify the validity and applicability of the model, Li *et al.* applied the model to simulate the shape memory performance under different loading modes and different boundary conditions. The simulation results are consistent with the experimental results, indicating that the model is suitable for different types of SMPs. This model can be used not only to predict the strain or stress response of SMPs under the free strain condition, but also to reproduce the shape memory behaviors under various flexible external constraints.

4.3. *Constitutive models combining viscoelasticity and phase transitions for SMPs*

We have discussed several representative models of SMPs on the basis of two constitutive modeling approaches, and each approach possesses obvious strengths and weakness. Intending to overcome the disadvantages, researchers combined both the viscoelastic and the phase transition theories together to establish a new framework of constitutive models for SMPs.

Based on multiplicative decompositions of the deformation gradient, Li *et al.* [2017a] proposed a novel phase transition-based viscoelastic model for SMPs which also includes the time-factor. Here, the definition of the molecular mechanism of SMPs is similar to the concepts of Leng *et al.* [2011], in which the network of SMPs is crosslinked and reoriented under an external load, where a reversible phase (secondary crosslinks) will appear during the cooling process to lock the deformed shape which then disappears at the heating recovery stage. To depict this mechanism, different constitutive structures for temperatures above and below glass transition T_g were defined separately, as presented in Fig. 13.

In this model, the rubbery phase is treated as a simple isotropic incompressible hyperplastic material which also considers the stress relaxation and creep due to sustained loading condition. Therefore, referring to Fig. 13(a), two incompressible hyperplastic elements and one viscous damper were introduced to represent the SMP model in the rubbery phase ($T > T_g$). (i.e., rubbery phase branch). In the glassy phase, a new reversible phase (the secondary cross-links) is initiated which acts to lock the temporary shape while temperature is below T_g. As presented in Fig. 13(b), springs in parallel with a viscous damper is applied to represent the
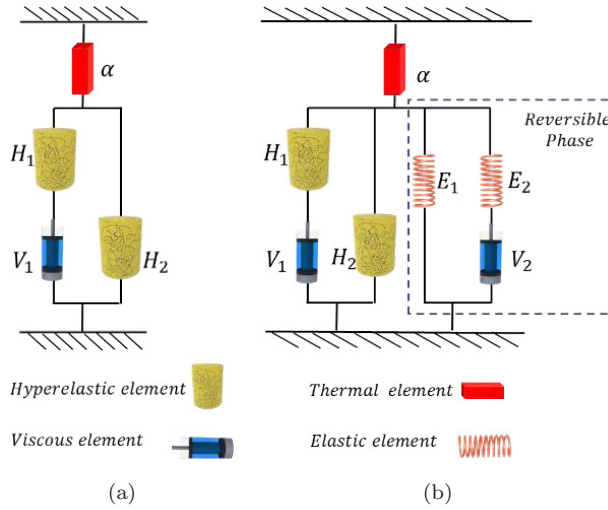
Fig. 13.   Schematic representation of the proposed constitutive model: (a) Constitutive model for SMPs at $T > T_g$ (rubbery state) and (b) constitutive model for SMPs at $T \leq T_g$ (glassy state).

secondary crosslinks or the reversible phase branch. Therefore, the SMP model at glassy phase ($T \leq T_g$) is a combination of the rubbery phase branch and the reversible phase branch. The detailed expressions of the total deformation gradient for both rubbery phase and glassy phase are given by Eqs. (2.5)–(2.7).

Accordingly, the Cauchy stress $\boldsymbol{\sigma}$ of each phase can be decomposed as the combination of different elements as

$$\begin{cases} \sigma = \sigma_{R1} + \sigma_{R2} & \text{(Rubbery phase } (T > Tg)) \\ \sigma = \sigma_{R1} + \sigma_{R2} + \sigma_{E1} + \sigma_{E2} & \text{(Glassy phase } (T \leq Tg)). \end{cases} \quad (4.24)$$

In order to depict the different structures of the model at each phase, the deformation state of each phase is treated separately. In general, the classic Mooney–Rivlin model is introduced to represent the free energy of the shape memory at the rubbery phase branch, while the Hencky strain definition is incorporated to derive the deformation gradient at the reversible phase branch [Bruhns *et al.*, 2002; Hencky, 1928]. The final constitutive equations are too convoluted; and hence will not be presented here. This work was further calibrated with test data from polyurethane SMP and Veriflex-E epoxy SMP, and the shape memory behaviors with different pre-strain level under multiple loading cases were analyzed. The simulation results proved this model could provide a good prediction for both small and large strain cases as well as wide validity for various SMPs. This relatively comprehensive constitutive model is not only able to embody the phase transition concept, but can also describe the viscoelastic characteristics of SMPs.

The previous model is based on the assumption that the secondary phase will appear or disappear under certain stimulus. However, further studies of polymer phase transitions revealed that phase transition can occur numerous times due to

the transformation between two or multiple phases. To address this, a novel model was further developed with the combination of the viscoelasticity and the phase transition [Li and Liu, 2018]. In this model, the SMP was considered as a mixture of rubbery phase and glassy phase. However, the rubbery phase is no longer treated as an elastic material but a viscoelastic material, which is represented by a standard Kelvin element and a spring element in series. For glassy phase at low temperature, since most molecular chains of SMPs are in frozen state, the model is expressed as a simple spring element, and the viscosity is ignored. The volume fraction of each phase can be visualized as the number of domains in each phase and varies with changes in temperature. The detailed structures of the proposed model are presented in Fig. 14.

Following the similar derivation process of the earlier model discussed in Sec. 4.2.2, the total stress and strain of this proposed model can be expressed as follows:

$$
\begin{cases}
\varepsilon_{\text{total}} = \Sigma\Delta\gamma_r^j(\varepsilon_{r1} + \varepsilon_{r2}^j) + \Sigma\Delta\gamma_g^j(\varepsilon_{g-\text{mechanics}} + \varepsilon_{\text{frozen}}^j) + \varepsilon_T \\
\sigma_{\text{total}} = \sigma_r^j = \sigma_g^j \\
\sigma_r^j = E_{r1}\varepsilon_{r1}^j = E_{r2}\varepsilon_{r2}^j + \eta\dot{\varepsilon}_{r2}^j, \quad \sigma_g^j = E_g\varepsilon_{g-\text{mechanics}}^j,
\end{cases}
\tag{4.25}
$$

where $\Delta\gamma_r^j$ and $\Delta\gamma_g^j$ denote the volume fraction of the jth rubbery phase and glassy phase. ε_{r1}, $\dot{\varepsilon}_{r2}^j$, $\varepsilon_{g-\text{mechanics}}$, $\varepsilon_{\text{frozen}}^j$ and ε_T denote the strain of two springs of the jth rubbery state, the residual mechanical strain, the frozen strain in the jth glassy state, and the total thermal strain, respectively. E_{r1}, E_{r2}, E_g are the Young's moduli of the springs in the rubbery and glassy states, and η the viscosity of the viscous damping element in the rubbery state. In the article, an evolution equation for each step of a SMP thermomechanical cycle was developed, and the model parameters were calibrated with a series of experimental data including isothermal uniaxial tensile test and stress relaxation test. This model could capture the critical features of SMP mechanical behavior as well as the rate-dependency of polymers and provide a credible description of experimental results of a polyurethane SMP under different pre-strains. In particular, the proposed model could fully embody the effects of four factors (stress relaxation, frozen strain, thermal strain, and Young's modulus) on
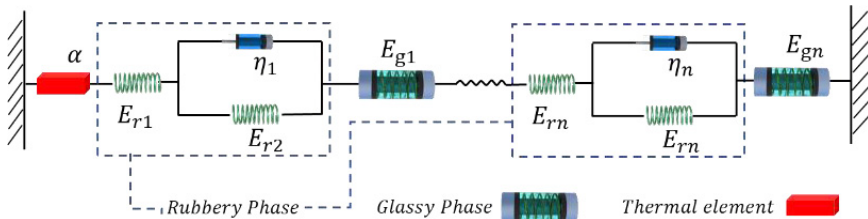

Fig. 14.   Schematic representation of the proposed constitutive model: SMPs are assumed to be composed of thermal element and two types of phase elements. The ratio of these two kinds of phase elements varies with the instantaneous temperature.

the stress evolution of the cooling step during a SMP cycle. Even so, by considering the glassy state as a pure-elastic polymer, the proposed model is only applicable for small deformation, which somewhat dampened its mainstream adoption.

5. Discussion on Different Constitutive Models

In Sec. 3, the constitutive models of hydrogels are presented in detail. Classified by their different environmental stimuli, the models can be divided into neutral gel, salt concentration-sensitive gel, pH-sensitive gel, temperature-sensitive gel, photo-thermal sensitive gel and magnetic sensitive gel. Although their theoretical formulations share the same basic formulas, their models are different by considering each respective distinctive free energy density part.

The neutral gel constitutive model is the fundamental model which other models are built upon. It is a model coupling the diffusion and large deformation theory. The biggest difference in the other models is the consideration for the different free energy density parts. The constitutive model of the salt concentration-sensitive gel is constructed by adding a mixing term of the solvent and ions to the basic free energy density, which considers the stretching of the network and mixing of the polymer chains and the solvent. Based on the model of salt concentration-sensitive gel, the model of pH-sensitive hydrogel was formulated by introducing another free energy density part, that of dissociating the acidic groups. The model of temperature-sensitive gel shares the same free energy density function with the neutral gel, but the interaction parameter χ is associated with the change of temperature. The model of photo-thermal sensitive gel was developed by including the part on photochemical reaction. Finally, the model of magnetic sensitive gel was proposed by adding a term due to the magnetization.

In Sec. 4, the constitutive models of SMPs were introduced in some detail. Since the intrinsic mechanisms of thermal-induced SMPs are largely similar with other types of SMPs triggered by different stimuli, we will thus in this paper here mainly review the theories for the thermal induced SMP. Generally, the constitutive models can be classified as rheological models or phenomenological phase transition models. Based on the viscoelasticity theories of polymers, rheological models of SMPs can be simply expressed within the spring-dashpot framework. However, these basic viscoelastic models cannot quantitively describe the thermomechanical behaviors of the SMPs, and researchers subsequently improved the models by introducing nonlinear terms and considering the rate and temperature dependence effects. Overall, rheological models could provide accurate predictions of thermomechanical performance including rate and temperature dependency of SMPs with complicated model parameters which need be fitted through experimental curves. The classical phenomenological model based on the phase translation approach was proposed following scrutiny of considerable experimental data and deep insight into the molecular mechanisms of the shape memory effect. [Liu *et al.*, 2006] considered the epoxy-based SMPs as a mixture of frozen and active phases, and the

volume fractions of the two phases could transform according to the temperature. This method has a clear physical interpretation; however, it only applies to certain types of SMPs. Consequently, researchers further developed this approach for large deformation behaviors of SMPs as well as considering the rate dependency in their specific models. Finally, several new constitutive models which made the effort to combine both advantages of rheological model and phenomenological models were introduced. The framework of this model type is analogous to that of the viscoelastic models of SMPs, and researchers need only to define multiple phases respectively in the whole system.

In order to realize hydrogel and SMP based engineering applications, the modeling and simulation methodology offers very useful approaches for investigating the deformation behaviors of hydrogel and SMP structures. For neutral gels, salt concentration-sensitive gel, pH-sensitive hydrogel and temperature sensitive gels,

Table 2. Constitutive equations of hydrogels under different external stimuli.

Type of hydrogel	Main constitutive equations of gel	Remark
Neutral gel	$\frac{s_{iK}}{kT/v} = Nv(F_{iK} - H_{iK}) + [J\log(1 - \frac{1}{J})$ $+ 1 + \frac{\chi}{J} - \frac{\mu}{kT}J]H_{iK}$	Hong *et al.* [2009]
Salt concentration-sensitive gel	$\frac{\sigma_{ij}}{\frac{kT}{v}} = \frac{Nv}{J}(F_{iK}F_{jK} - \delta_{ij})$ $+ (\log\frac{J-1}{J} + \frac{1}{J} + \frac{\chi}{J^2} + 2\nu c_0)\delta_{ij}$ $+ \nu\delta_{ij}[c^+(\log\frac{c^+}{c_0} - 1) + c^-(\log\frac{c^-}{c_0} - 1)$ $+ J(\frac{\partial c^+}{\partial J}\log\frac{c^+}{c_0} + \frac{\partial c^-}{\partial J}\log\frac{c^-}{c_0})]$	Zheng and Liu [2019]
pH-sensitive gel	$\frac{\sigma_{ij}}{kT/v} = \frac{Nv}{J}(F_{iK}F_{jK} - \delta_{ij})$ $+ (\log\frac{J-1}{J} + \frac{1}{J} + \frac{\chi}{J^2})\delta_{ij}$ $- \nu\delta_{ij}[c^{H^+} + c^+ + c^-$ $- \bar{c}^{H^+} - \bar{c}^+ - \bar{c}^-]$	Marcombe *et al.* [2010]
Temperature-sensitive gel	$N\nu(\lambda_1^2 - 1) + (\frac{V}{V_0})\log[1 - (\frac{V}{V_0})^{-1}] + 1$ $+ (\chi_0 - \chi_1)(\frac{V}{V_0})^{-1} + 2\chi_1(\frac{V}{V_0})^{-2} = 0,$ $\frac{1}{\lambda_3}[N\nu(\lambda_3^2 - 1) + (\frac{V}{V_0})\log[1 - (\frac{V}{V_0})^{-1}] + 1$ $+ (\chi_0 - \chi_1)(\frac{V}{V_0})^{-1} + 2\chi_1(\frac{V}{V_0})^{-2}] = \frac{s\nu}{kT}$	Ding *et al.* [2013, 2016]
Photo-thermal sensitive gel	$\frac{\sigma_{ij}}{\frac{kT}{v}} = \frac{Nv}{J}(F_{iK}F_{jK} - \delta_{ij})$ $+ (\log\frac{J-1}{J} + \frac{1}{J} + \frac{\chi_0 - \chi_1}{J^2} + \frac{\chi_1}{J^3})\delta_{ij}$ $+ \nu\frac{\alpha I_0}{hf}[\frac{2(c^{(\text{network})} - c^{(w)})}{J^3} + \frac{c^{(w)}}{J^2}]\delta_{ij}$ $- \frac{\mu}{kT}\delta_{ij}$	Toh *et al.* [2014a]
Magnetic-sensitive gel	$\frac{s_{ik}\nu}{kT_0} = N\nu\frac{T}{T_0}(F_{iK} - H_{iK}) + \frac{T}{T_0}[\ln(\frac{J-1}{J})$ $+ \frac{1}{J} + \frac{\chi_0 - \chi_1}{J^2} + \frac{2\chi_1}{J^3}]JH_{iK}$ $- \bar{\mu}^s JH_{iK} + N_m\nu f_m\frac{\bar{B}\tanh(\bar{B}\frac{T_0}{T})}{J^2}JH_{iK}$	Hu *et al.* [2018a], Zhao *et al.* [2019]

Table 3. The constitutive models of thermal-induced SMPs.

Category	Type of models	Main constitutive equations of SMP	Remark
Rheological models of SMP	Basic viscoelastic model	$\sigma + \frac{\mu(T)}{(E_1(T)+E_2(T))}\frac{d\sigma}{dt}$ $= \frac{\mu(T)}{(1+E_1(T)/E_2(T))}\left(\frac{d\varepsilon}{dt} - \alpha\frac{dT}{dt}\right)$ $+ \frac{1}{(1/E_1(T)+1/E_2(T))}(\varepsilon - \alpha(T-T_0))$	Li *et al.* [2015]
	Thermoviscoelastic models of SMPs coupled with temperature and rate effects	$\boldsymbol{\sigma}^n = \frac{E_r^n}{6}\frac{T}{T_h}\mathbf{F}^e\mathbf{F}e^T - p\mathbf{I}$ from entropy branch $\boldsymbol{\sigma}^U = \mathbf{L}^e[\ln(\mathbf{V}^e)]$ from internal energy branch	Diani *et al.* [2006]
	Fractional viscoelastic constitutive model	$\sigma_M(t) = \sigma_{eq}(t) + \sum_{i=1}^m \sigma_i(t)$ $= E_{eq}\varepsilon_M(t)$ $+ \sum_{i=1}^2 \left[E_i \int_{t_0}^t E_\beta\left(-\left(\frac{t-\xi}{\tau_i}\right)^\beta\right)\frac{d\varepsilon_M(\xi)}{d\xi}\, d\xi \right.$ $\left. + E_\beta\left(-\left(\frac{t-t_0}{\tau_i}\right)^\beta\right)\sigma_i(t_0)\right]$	Pan and Liu [2018]
Phenomenological models of SMP	Classic phenomenological constitutive model	$\boldsymbol{\sigma} = \frac{\boldsymbol{\varepsilon} - \boldsymbol{\varepsilon}_s - \boldsymbol{\varepsilon}_T}{\frac{\phi_f}{E_i} + \frac{1-\phi_f}{E_e}} = E(\boldsymbol{\varepsilon} - \boldsymbol{\varepsilon}_s - \int_{T_h}^T \alpha dT)$	Liu *et al.* [2006]
	Phenomenological models of SMP considering rate effect	$\sigma_{\text{total}} = \frac{\varepsilon_{\text{total}} - \varepsilon_{f-\text{real}} - \varepsilon_T}{\frac{\gamma}{E_g} + \frac{1-\gamma}{E_r}}$ $\frac{d\varepsilon_f}{dT} = \frac{d\gamma}{dT}[1 - f(T)]\frac{\varepsilon_{\text{total}} - \varepsilon_f - \varepsilon_T}{E_r\left(\frac{\gamma}{E_g} + \frac{1-\gamma}{E_r}\right)}$ $\varepsilon_{f-\text{real}} = \varepsilon_f - \int_0^t \dot\varepsilon_f e^{\frac{-(t-a)}{\tau}}\, da$	Li *et al.* [2017a, 2007b]
Combined viscoelasticity & phase transitions model for SMPs	Model considering viscoelasticity & phase transition	$\varepsilon_{\text{total}} = \sum\Delta\gamma_r^j(\varepsilon_{r1} + \varepsilon_{r2}^j)$ $+ \sum\Delta\gamma_g^j(\varepsilon_{g-\text{mechanics}} + \varepsilon_{\text{frozen}}^j) + \varepsilon_T$ $\sigma_{\text{total}} = \sigma_r^j = \sigma_g^j$ $\sigma_r^j = E_{r1}\varepsilon_{r1}^j = E_{r2}\varepsilon_{r2}^j + \eta\dot\varepsilon_{r2}^j,$ $\sigma_g^j = E_g\varepsilon_g^j|_{g-\text{mechanics}}$	Li and Liu [2018]

the robust finite element method (FEM) as well as meshless methods have been proposed [Ding *et al.*, 2013; Hong *et al.*, 2009; Liu and Cheng, 2018; Liu *et al.*, 2019a; Zheng and Liu, 2019] and these methods can correctly predict the deformation behavior and deformation mechanism of hydrogel structures. However, for photo-thermal sensitive gel and magnetic sensitive gel, there remains much work to be done in the implementation of the constitutive models into FEM. It is also imperative to propose efficient numerical schemes to study the deformation of complex structures of photo-thermal sensitive gel and magnetic sensitive gel. For above discussed hydrogel constitutive models, the constitutive equations are summarized in Table 2. For SMP constitutive models, as they involve different phases and time history. Proper FEM implementations are currently available only for a few limited cases, such as the simplified three-element model, the phase-evolution-based thermomechanical constitutive model, etc. Thus, their implementation as a user material subroutine in a finite element solver package, such as UMAT in ABAQUS, still requires some coding efforts. For different thermal-induced SMP constitutive models, the constitutive equations are summarized in Table 3, which will be useful for numerical implementation.

6. Potential Applications of Constitutive Models and Some Research Gaps

In this Review, we have systematically introduced the constitutive models of hydrogels and SMPs. A good perception towards the mechanics of hydrogels is crucial for future applications, especially in the areas of soft robotics and soft material adhesion problems [Yang *et al.*, 2019]. For example, magnetically responsive soft robots made of hydrogels have achieved noteworthy flexibility and controllability [Kim *et al.*, 2018]. However, the constitutive model of magnetic sensitive hydrogel has not been applied to exploit its full capabilities yet. It is believed that a combination of constitutive modelling and synthesis methods of magnetically responsive soft robots will increased the range of the usage of these soft robots. In addition, soft material adhesion problems have attracted the attention of many research groups recently. Even so, current research is still unable to integrate adhesion effects into the hydrogel constitutive models. It is our hope that more comprehensive constitutive models can be developed soon to advance the resolution of hydrogel adhesion problems.

Moreover, there are some research gaps in the constitutive modelling of hydrogels. As mentioned in Sec. 3, the current study of pH-sensitive hydrogel still assumes C^a to be independent of J. As stated in Sec. 3.2, this assumption is problematic as it cannot be properly implemented as an ABAQUS subroutine. Future studies may focus on new pH-sensitive hydrogel models which assume C^a to be dependent of J. Furthermore, the constitutive models of magnetic sensitive hydrogel are still pending verification against experimental data. There is seemingly limited reported experimental works directed towards the characterization of mechanical behaviors of hydrogels.

Regarding SMPs, we have discussed several widely used constitutive SMP models which can be adopted in diverse applications for different situations. However, many remaining issues still need to be resolved. Generally, the different working conditions exert differing effects on the overall mechanical properties of SMPs. Under certain specific application conditions, the earlier proposed constitutive equations with simplified assumptions sometimes cannot precisely predict the SMP performance. For example, when introducing SMPs as a vascular stent into the human body, the vessel will exert unpredictable loading conditions on the stent. In order to carry out precise numerical modelling and simulation, the complex blood flow dynamics, triggering mechanisms of the stent and the shape memory effect must be taken into account and be extensively investigated [Liu *et al.*, 2019e].

Also, current established theories have focused on temperature sensitive SMPs, while the constitutive models applied to the photo-sensitive and magneto-sensitive type shape memory polymers can be considered to be still in the development stage. Meanwhile, SMPs have some distinctive weaknesses, such as low recovery stress, which also restricts the applications of SMPs in smart soft robotic systems. In general, proposing innovative approaches that could exploit the special attributes of SMPs in an optimum manner, as well as improving the current SMP structures to achieve higher levels of performance should be the future directions of the research community and industry.

Although some robust constitutive models for hydrogels and SMPs have been proposed and discussed in Secs. 1–5, most of their utilization is still limited to 1D or 2D simulation cases. Therefore, the implementation of these constitutive modes into the FEM or other numerical approaches will be imperative. For example: for hydrogels, the kinetic predictions of deformation behaviors are still fairly preliminary; for SMPs, establishing efficient numerical approaches for SMP structure deformation procedures is crucial.

Since these smart hydrogel and SMP materials may be concurrently activated under multiple stimuli, the coupling of their constitutive models should be further developed. This will facilitate more extensive applications of hydrogels and SMPs in the future.

7. Concluding Remarks

This paper has been written with the aim of strengthening conceptual understanding and ideas related to recent advances of the constitutive models of hydrogels and SMPs. Many hydrogel types have been explored, with attention given more to the monophase theories for its unifying approach by adding different free energy density parts. Three main types of SMPs have been introduced in this paper, with much emphasis given to their rheology, phase transition and viscoelasticity. With better understanding of the mechanics of hydrogels and SMPs, it is possible to develop novel applications which possess superior performance over current conventional engineering materials. We hope this review paper will provide researchers

involved in the mechanics of soft materials with the basic guidelines for their further investigations into hydrogels and SMPs, as well as their efforts in the research and development of soft machines.

Acknowledgment

References

Afroze, F., Nies, E. and Berghmans, H. [2000] "Phase transitions in the system poly (N-isopropylacrylamide)/water and swelling behaviour of the corresponding networks," *Journal of Molecular Structure* **554**(1), 55–68.

Augst, A. D., Kong, H. J. and Mooney, D. J. [2006] "Alginate hydrogels as biomaterials," *Macromolecular Bioscience* **6**(8), 623.

Baghani, M., Arghavani, J. and Naghdabadi, R. [2014] "A finite deformation constitutive model for shape memory polymers based on Hencky strain," *Mechanics of Materials* **73**(1), 1–10.

Baghani, M., Naghdabadi, R., Arghavani, J. and Sohrabpour, S. [2012] "A thermodynamically-consistent 3D constitutive model for shape memory polymers," *International Journal of Plasticity* **35**, 13–30.

Bai, R., Yang, Q., Tang, J., Morelle, X. P., Vlassak, J. and Suo, Z. [2017] "Fatigue fracture of tough hydrogels," *Extreme Mechanics Letters* **15**, 91–96.

Barot, G. and Rao, I. J. [2006] "Constitutive modeling of the mechanics associated with crystallizable shape memory polymers," *Zeitschrift Fur Angewandte Mathematik Und Physik* **57**(4), 652–681.

Behl, M., Razzaq, M. Y. and Lendlein, A. [2010] "Multifunctional shape-memory polymers," *Advanced Materials* **22**(31), 3388–3410.

Birgersson, E., Li, H. and Wu, S. [2008] "Transient analysis of temperature-sensitive neutral hydrogels," *Journal of the Mechanics and Physics of Solids* **56**(2), 444–466.

Bouklas, N., Landis, C. M. and Huang, R. [2015] "Effect of solvent diffusion on crack-tip fields and driving force for fracture of hydrogels," *Journal of Applied Mechanics-Transactions of the ASME* **82**(8), 081007.

Boyce, M. C. and Arruda, E. M. [2000] "Constitutive models of rubber elasticity: A review," *Rubber Chemistry and Technology* **73**(3), 504–523.

Bruhns, O. T., Xiao, H. and Meyers, A. [2002] "Finite bending of a rectangular block of an elastic hencky material," *Journal of Elasticity and the Physical Science of Solids* **66**(3), 237–256.

Buckley, C. P., Prisacariu, C. and Caraculacu, A. [2007] "Novel triol-crosslinked polyurethanes and their thermorheological characterization as shape-memory materials," *Polymer* **48**(5), 1388–1396.

Cai, S. and Suo, Z. [2011] "Mechanics and chemical thermodynamics of phase transition in temperature-sensitive hydrogels," *Journal of the Mechanics and Physics of Solids* **59**(11), 2259–2278.

Castro, F., Westbrook, K. K., Long, K. N., Shandas, R. and Qi, H. J. [2010] "Effects of thermal rates on the thermomechanical behaviors of amorphous shape memory polymers," *Mechanics of Time-Dependent Materials* **14**(3), 219–241.

Chen, Y.-C. and Lagoudas, D. C. [2008a] "A constitutive theory for shape memory polymers. Part I," *Journal of the Mechanics and Physics of Solids* **56**(5), 1752–1765.

Chen, Y.-C. and Lagoudas, D. C. [2008b] "A constitutive theory for shape memory polymers. Part II," *Journal of the Mechanics and Physics of Solids* **56**(5), 1766–1778.

Chester, S. A. and Anand, L. [2010] "A coupled theory of fluid permeation and large deformations for elastomeric materials," *Journal of the Mechanics and Physics of Solids* **58**(11), 1879–1906.

Chester, S. A. and Anand, L. [2011] "A thermo-mechanically coupled theory for fluid permeation in elastomeric materials: Application to thermally responsive gels," *Journal of the Mechanics and Physics of Solids* **59**(10), 1978–2006.

Dai, L., Tian, C. and Xiao, R. [2020] "Modeling the thermo-mechanical behavior and constrained recovery performance of cold-programmed amorphous shape-memory polymer," *International Journal of Plasticity* **127**, 102654.

Di Marzio, E. A. and Yang, A. J. M. [1997] "Configurational entropy approach to the kinetics of glasses," *Journal of Research of the National Institute of Standards and Technology* **102**(2), 135–157.

Diani, J., Liu, Y. P. and Gall, K. [2006] "Finite strain 3D thermoviscoelastic constitutive model for shape memory polymers," *Polymer Engineering and Science* **46**(4), 486–492.

Ding, Z., Liu, Z., Hu, J., Swaddiwudhipong, S. and Yang, Z. [2013] "Inhomogeneous large deformation study of temperature-sensitive hydrogel," *International Journal of Solids and Structures* **50**(16–17), 2610–2619.

Ding, Z., Toh, W., Hu, J., Liu, Z. and Ng, T. Y. [2016] "A simplified coupled thermo-mechanical model for the transient analysis of temperature-sensitive hydrogels," *Mechanics of Materials* **97**, 212–227.

Drozdov, A. [2014] "Swelling of thermo-responsive hydrogels," *The European Physical Journal E* **37**(10), 93.

Drozdov, A. and Christiansen, J. D. [2017] "Mechanical response and equilibrium swelling of temperature-responsive gels," *European Polymer Journal* **94**, 56–67.

Drozdov, A., Sanporean, C.-G. and Christiansen, J. D. [2015] "Modeling the effects of temperature and pH on swelling of stimuli-responsive gels," *European Polymer Journal* **73**, 278–296.

Drury, J. L. and Mooney, D. J. [2003] "Hydrogels for tissue engineering: Scaffold design variables and applications," *Biomaterials* **24**(24), 4337–4351.

Flory, P. J. [1942] "Thermodynamics of high polymer solutions," *The Journal of Chemical Physics* **10**(1), 51–61.

Flory, P. J. and Rehner, J. [1943] "Statistical mechanics of cross-linked polymer networks I. Rubberlike elasticity," *The Journal of Chemical Physics* **11**(11), 512–512.

Ghosh, P. and Srinivasa, A. R. [2013] "A two-network thermomechanical model and parametric study of the response of shape memory polymers," *Mechanics of Materials* **60**, 1–17.

Gong, J. P. [2010] "Why are double network hydrogels so tough?," *Soft Matter* **6**(12), 2583–2590.

Gong, J. P., Katsuyama, Y., Kurokawa, T. and Osada, Y. [2003] "Double-network hydrogels with extremely high mechanical strength," *Advanced Materials* **15**(14), 1155–1158.

Gu, J., Sun, H. and Fang, C. [2015] "A phenomenological constitutive model for shape memory polyurethanes," *Journal of Intelligent Material Systems and Structures* **26**(5), 517–526.

Hager, M. D., Bode, S., Weber, C. and Schubert, U. S. [2015] "Shape memory polymers: Past, present and future developments," *Progress in Polymer Science* **49–50**, 3–33.

Hamzavi, N., Drozdov, A. D., Gu, Y. and Birgersson, E. [2016] "Modeling equilibrium swelling of a dual pH- and temperature-responsive core/shell hydrogel," *International Journal of Applied Mechanics* **08**(3), 1650039.

He, Y., Guo, S., Liu, Z. and Liew, K. M. [2015] "Pattern transformation of thermo-responsive shape memory polymer periodic cellular structures," *International Journal of Solids and Structures* **71**, 194–205.

He, Y., Li, Y., Liu, Z. and Liew, K. M. [2017a] "Buckling analysis and buckling control of thin films on shape memory polymer substrate," *European Journal of Mechanics A-Solids* **66**, 356–369.

He, Y., Zhou, Y., Liu, Z. and Liew, K. M. [2017b] "Pattern transformation of single-material and composite periodic cellular structures," *Materials and Design* **132**, 375–384.

He, Y., Zhou, Y., Liu, Z. and Liew, K. M. [2018] "Buckling and pattern transformation of modified periodic lattice structures," *Extreme Mechanics Letters* **22**, 112–121.

Hencky, H. [1928] "Über die Form des Elastizitätsgesetzes bei ideal elastischen Stoffen," *Z. Techn. Phys.* **9**, 215–220.

Hong, W., Liu, Z. and Suo, Z. [2009] "Inhomogeneous swelling of a gel in equilibrium with a solvent and mechanical load," *International Journal of Solids and Structures* **46**(17), 3282–3289.

Hong, W., Zhao, X., Zhou, J. and Suo, Z. [2008] "A theory of coupled diffusion and large deformation in polymeric gels," *Journal of the Mechanics and Physics of Solids* **56**(5), 1779–1793.

Hu, J., He, Y., Lei, J. and Liu, Z. [2013] "Novel mechanical behavior of periodic structure with the pattern transformation," *Theoretical and Applied Mechanics Letters* **3**(5), 054007.

Hu, J., He, Y., Lei, J., Liu, Z. and Swaddiwudhipong, S. [2014] "Mechanical behavior of composite gel periodic structures with the pattern transformation," *Structural Engineering and Mechanics* **50**(5), 605–616.

Hu, J., Toh, W. and Liu, Z. [2018a] "Study on deformation behavior of magneto-thermal sensitive hydrogels," *Proceedings of 2018 National Conference on Solid Mechanics*, 23–25 Nov., Harbin, China, p. 1.

Hu, J., Zhou, Y. and Liu, Z. [2018b] "The friction effect on buckling behavior of cellular structures under axial load," *International Journal of Applied Mechanics* **10**(2), 1850013.

Hu, J., Zhou, Y., Liu, Z. and Ng, T. Y. [2017] "Pattern switching in soft cellular structures and hydrogel-elastomer composite materials under compression," *Polymers* **9**(6), 229.

Hu, J. L. and Chen, S. J. [2010] "A review of actively moving polymers in textile applications," *Journal of Materials Chemistry* **20**(17), 3346–3355.

Hu, J. L., Zhu, Y., Huang, H. H. and Lu, J. [2012] "Recent advances in shape-memory polymers: Structure, mechanism, functionality, modeling and applications," *Progress in Polymer Science* **37**(12), 1720–1763.

Huggins, M. L. [1941] "Solutions of long chain compounds," *The Journal of Chemical Physics* **9**(5), 440–440.

Huggins, M. L. [1964] "A revised theory of high polymer solutions," *Journal of the American Chemical Society* **86**(17), 3535–3540.

Kim, Y., Yuk, H., Zhao, R., Chester, S. A. and Zhao, X. [2018] "Printing ferromagnetic domains for untethered fast-transforming soft materials," *Nature* **558**(7709), 274.

Lendlein, A., Behl, M., Hiebl, B. and Wischke, C. [2010] "Shape-memory polymers as a technology platform for biomedical applications," *Expert Review of Medical Devices* **7**(3), 357–379.

Leng, J., Xin, L., Liu, Y. and Du, S. [2011] "Shape-memory polymers and their composites: Stimulus methods and applications," *Progress in Materials Science* **56**(7), 1077–1135.

Leng, J. S., Lu, H. B., Liu, Y. J., Huang, W. M. and Du, S. Y. [2009] "Shape-memory polymers — A class of novel smart materials," *Mrs Bulletin* **34**(11), 848–855.

Li, H. and Lai, F. [2010] "Multiphysics modeling of responsive characteristics of ionic-strength-sensitive hydrogel," *Biomedical Microdevices* **12**(3), 419–434.

Li, H., Luo, R., Birgersson, E. and Lam, K. Y. [2007a] "Modeling of multiphase smart hydrogels responding to pH and electric voltage coupled stimuli," *Journal of Applied Physics* **101**(11), 114905.

Li, H., Luo, R. and Lam, K. Y. [2007b] "Modeling and simulation of deformation of hydrogels responding to electric stimulus," *Journal of Biomechanics* **40**(5), 1091–1098.

Li, H., Luo, R. and Lam, K. Y. [2007c] "Modeling of ionic transport in electric-stimulus-responsive hydrogels," *Journal of Membrane Science* **289**(1–2), 284–296.

Li, H., Ng, T. Y., Yew, Y. K. and Lam, K. Y. [2005] "Modeling and simulation of the swelling behavior of pH-stimulus-responsive hydrogels," *Biomacromolecules* **6**(1), 109–120.

Li, H., Ng, T. Y., Yew, Y. K. and Lam, K. Y. [2007d] "Meshless modeling of pH-sensitive hydrogels subjected to coupled pH and electric field stimuli: Young modulus effects and case studies," *Macromolecular Chemistry and Physics* **208**(10), 1137–1146.

Li, Y., Liu, R. and Liu, Z. [2018] "The dynamic behaviors of a shape memory polymer membrane," *Acta Mechanica Solida Sinica* **31**(5), 635–651.

Li, Y. X., Guo, S. S., He, Y. H. and Liu, Z. S. [2015] "A simplified constitutive model for predicting shape memory polymers deformation behavior," *International Journal of Computational Materials Science and Engineering* **4**(1), 1550001.

Li, Y. X., He, Y. H. and Liu, Z. S. [2017a] "A viscoelastic constitutive model for shape memory polymers based on multiplicative decompositions of the deformation gradient," *International Journal of Plasticity* **91**, 300–317.

Li, Y. X., Hu, J. Y. and Liu, Z. S. [2017b] "A constitutive model of shape memory polymers based on glass transition and the concept of frozen strain release rate," *International Journal of Solids and Structures* **124**, 252–263.

Li, Y. X. and Liu, Z. S. [2018] "A novel constitutive model of shape memory polymers combining phase transition and viscoelasticity," *Polymer* **143**, 298–308.

Li, Z. and Liu, Z. [2019] "Energy transfer speed of polymer network and its scaling-law of elastic modulus — New insights," *Journal of Applied Physics* **126**(21), 215101.

Li, Z., Liu, Z., Ng, T. Y. and Sharma, P. [2019] "The effect of water content on the elastic modulus and fracture energy of hydrogel," *Extreme Mechanics Letters*, 100617 (in Press).

Liu, F. and Cheng, Y. [2018] "The improved element-free Galerkin method based on the nonsingular weight functions for inhomogeneous swelling of polymer gels," *International Journal of Applied Mechanics* **10**(4), 1850047.

Liu, F., Wu, Q. and Cheng, Y. [2019a] "A meshless method based on the nonsingular weight functions for elastoplastic large deformation problems," *International Journal of Applied Mechanics* **11**(1), 1950006.

Liu, J., Yang, C., Yin, T., Wang, Z., Qu, S. and Suo, Z. [2019b] "Polyacrylamide hydrogels. II. Elastic dissipater," *Journal of the Mechanics and Physics of Solids* **133**, 103737.

Liu, Q., Li, H. and Lam, K. Y. [2019c] "Modeling of a fast-response magnetic-sensitive hydrogel for dynamic control of microfluidic flow," *Physical Chemistry Chemical Physics* **21**(4), 1852–1862.

Liu, R., Li, Y. and Liu, Z. [2019d] "Experimental study of thermo-mechanical behavior of a thermosetting shape-memory polymer," *Mechanics of Time-Dependent Materials* **23**(3), 249–266.

Liu, R. X., Mcginty, S., Cui, F. S., Luo, X. Y. and Liu, Z. S. [2019e] "Modelling and simulation of the expansion of a shape memory polymer stent," *Engineering Computations* **36**(8), 2726–2746.

Liu, Y., Du, H., Liu, L. and Leng, J. [2014] "Shape memory polymers and their composites in aerospace applications: A review," *Smart Materials and Structures* **23**(2), 023001.

Liu, Y. P., Gall, K., Dunn, M. L., Greenberg, A. R. and Diani, J. [2006] "Thermomechanics of shape memory polymers: Uniaxial experiments and constitutive modeling," *International Journal of Plasticity* **22**(2), 279–313.

Liu, Z. and Calvert, P. [2000] "Multilayer hydrogels as muscle-like actuators," *Advanced Materials* **12**(4), 288–291.

Liu, Z., Hong, W., Suo, Z., Swaddiwudhipong, S. and Zhang, Y. [2010] "Modeling and simulation of buckling of polymeric membrane thin film gel," *Computational Materials Science* **49**(1), S60–S64.

Liu, Z., Swaddiwudhipong, S. and Hong, W. [2013] "Pattern formation in plants via instability theory of hydrogels," *Soft Matter* **9**(2), 577–587.

Liu, Z. C., Chen, G. F., Liang, P., Zhang, J. Q., Cui, F. S. and Xu, M. L. [2017] "Biomechanical assessment for healing progression of fractured long bones: Numerical investigations of bending stiffness and resonant frequency," *International Journal of Applied Mechanics* **9**(3), 1750041.

Liu, Z. S., Toh, W. and Ng, T. Y. [2015] "Advances in mechanics of soft materials: A review of large deformation behavior of hydrogels," *International Journal of Applied Mechanics* **7**(5), 1530001.

Long, K. N., Dunn, M. L. and Qi, H. J. [2010] "Mechanics of soft active materials with phase evolution," *International Journal of Plasticity* **26**(4), 603–616.

Lu, H. B., Wang, X. D., Xiang, Z. Y. and Fu, Y. Q. [2019] "A cooperative domain model for multiple phase transitions and complex conformational relaxations in polymers with shape memory effect," *Journal of Physics D: Applied Physics* **52**(24).

Lu, H. B., Wang, X. D., Yao, Y. T. and Fu, Y. Q. [2018] "A 'frozen volume' transition model and working mechanism for the shape memory effect in amorphous polymers," *Smart Materials and Structures* **27**(6), 065023.

Luo, X. F. and Mather, P. T. [2013] "Shape memory assisted self-healing coating," *Acs Macro Letters* **2**(2), 152–156.

Marcombe, R., Cai, S., Hong, W., Zhao, X., Lapusta, Y. and Suo, Z. [2010] "A theory of constrained swelling of a pH-sensitive hydrogel," *Soft Matter* **6**(4), 784–793.

Moon, S., Cui, F. and Rao, I. J. [2015] "Constitutive modeling of the mechanics associated with triple shape memory polymers," *International Journal of Engineering Science* **96**, 86–110.

Morshedian, J., Khonakdar, H. A. and Rasouli, S. [2005] "Modeling of shape memory induction and recovery in heat-shrinkable polymers," *Macromolecular Theory and Simulations* **14**(7), 428–434.

Ng, T. Y., Li, H., Yew, Y. K. and Lam, K. Y. [2007] "Effects of initial-fixed charge density on pH-sensitive hydrogels subjected to coupled pH and electric field stimuli: A meshless analysis," *Journal of Biomechanical Engineering-Transactions of the ASME* **129**(2), 148–155.

Nguyen, K. T. and West, J. L. [2002] "Photopolymerizable hydrogels for tissue engineering applications," *Biomaterials* **23**(22), 4307–4314.

Nguyen, T. D., Qi, H. J., Castro, F. and Long, K. N. [2008] "A thermoviscoelastic model for amorphous shape memory polymers: Incorporating structural and stress relaxation," *Journal of the Mechanics and Physics of Solids* **56**(9), 2792–2814.

Okumura, D. and Chester, S. A. [2018] "Ultimate swelling described by limiting chain extensibility of swollen elastomers," *International Journal of Mechanical Sciences* **144**, 531–539.

Pan, Z., Huang, R. and Liu, Z. [2019] "Prediction of the thermomechanical behavior of particle reinforced shape memory polymers," *Polymer Composites* **40**(1), 353–363.

Pan, Z., Zhou, Y., Zhang, N. and Liu, Z. [2018] "A modified phase-based constitutive model for shape memory polymers," *Polymer International* **67**(12), 1677–1683.

Pan, Z. Z. and Liu, Z. S. [2018] "A novel fractional viscoelastic constitutive model for shape memory polymers," *Journal of Polymer Science Part B-Polymer Physics* **56**(16), 1125–1134.

Qi, H. J., Nguyen, T. D., Castroa, F., Yakacki, C. M. and ShandaSa, R. [2008] "Finite deformation thermo-mechanical behavior of thermally induced shape memory polymers," *Journal of the Mechanics and Physics of Solids* **56**(5), 1730–1751.

Qiu, Y. and Park, K. [2001] "Environment-sensitive hydrogels for drug delivery," *Advanced Drug Delivery Reviews* **53**(3), 321–339.

Reese, S., Böl, M. and Christ, D. [2010] "Finite element-based multi-phase modelling of shape memory polymer stents," *Computer Methods in Applied Mechanics and Engineering* **199**(21), 1276–1286.

Shojaei, A., Li, G. Q. and Voyiadjis, G. Z. [2013] "Cyclic viscoplastic-viscodamage analysis of shape memory polymers fibers with application to self-healing smart materials," *Journal of Applied Mechanics-Transactions of the ASME* **80**(1), 011014.

Stöhr, J. and Siegmann, H. C. [2006] *Magnetism: From Fundamentals to Nanoscale Dynamics* (Springer Berlin/Heidelberg).

Sun, J., Zhao, X., Illeperuma, W. R., Chaudhuri, O., Oh, K. H., Mooney, D. J., Vlassak, J. J. and Suo, Z. [2012] "Highly stretchable and tough hydrogels," *Nature* **489**, 133–136.

Tobushi, H., Hara, H., Yamada, E. and Hayashi, S. [1996a] "Thermomechanical properties in a thin film of shape memory polymer of polyurethane series," *Smart Materials and Structures* **5**(4), 483–491.

Tobushi, H., Hashimoto, T., Hayashi, S. and Yamada, E. [1997] "Thermomechanical constitutive modeling in shape memory polymer of polyurethane series," *Journal of Intelligent Material Systems and Structures* **8**(8), 711–718.

Tobushi, H., Hayashi, S., Ikai, A. and Hara, H. [1996b] "Thermomechanical properties of shape memory polymers of polyurethane series and their applications," *Journal De Physique IV* **6**(C1), 377–384.

Tobushi, H., Okumura, K., Hayashi, S. and Ito, N. [2001] "Thermomechanical constitutive model of shape memory polymer," *Mechanics of Materials* **33**(10), 545–554.

Toh, W., Ding, Z., Ng, T. Y. and Liu, Z. [2015] "Wrinkling of a polymeric gel during transient swelling," *Journal of Applied Mechanics-Transactions of the ASME* **82**(6), 061004.

Toh, W., Ding, Z., Ng, T. Y. and Liu, Z. [2016] "Light intensity controlled wrinkling patterns in photo-thermal sensitive hydrogels," *Coupled Systems Mechanics* **5**(4), 315–327.

Toh, W., Liu, Z., Ng, T. Y. and Hong, W. [2013] "Inhomogeneous large deformation kinetics of polymeric gels," *International Journal of Applied Mechanics* **5**(1), 1350001.

Toh, W., Ng, T. Y., Hu, J. and Liu, Z. [2014a] "Mechanics of inhomogeneous large deformation of photo-thermal sensitive hydrogels," *International Journal of Solids and Structures* **51**(25–26), 4440–4451.

Toh, W., Ng, T. Y., Liu, Z. and Hu, J. [2014b] "Deformation kinetics of pH-sensitive hydrogels," *Polymer International* **63**(9), 1578–1583.

Wei, Z., Yang, J. H., Liu, Z. Q., Xu, F., Zhou, J. X., Zrínyi, M., Osada, Y. and Chen, Y. M. [2015] "Novel biocompatible polysaccharide-based self-healing hydrogel," *Advanced Functional Materials* **25**(9), 1352–1359.

Wu, T. and Li, H. [2018] "Phase-field model for liquid–solid phase transition of physical hydrogel in an ionized environment subject to electro–chemo–thermo–mechanical coupled field," *International Journal of Solids and Structures* **138**, 134–143.

Xiang, Y., Zhong, D., Wang, P., Mao, G., Yu, H. and Qu, S. [2018] "A general constitutive model of soft elastomers," *Journal of the Mechanics and Physics of Solids* **117**, 110–122.

Xiao, Y., Zhong, D., Wang, P., Yin, T., Zhou, H., Yu, H., Baliga, C., Qu, S. and Yang, W. [2019] "A physically based visco-hyperelastic constitutive model for soft materials," *Journal of the Mechanics and Physics of Solids* **128**, 208–218.

Xiao, R., Guo, J. and Nguyen, T. D. [2015] "Modeling the multiple shape memory effect and temperature memory effect in amorphous polymers," *RSC Advances* **5**(1), 416–423.

Xiao, R., Qian, J. and Qu, S. [2019] "Modeling gel swelling in binary solvents: A thermodynamic approach to explaining cosolvency and cononsolvency effects," *International Journal of Applied Mechanics* **11**(5), 1950050.

Xiao, R., Yakacki, C. M., Guo, J., Frick, C. P. and Nguyen, T. D. [2016] "A predictive parameter for the shape memory behavior of thermoplastic polymers," *Journal of Polymer Science Part B-Polymer Physics* **54**(14), 1405–1414.

Xu, D., Huang, J., Zhao, D., Ding, B., Zhang, L. and Cai, J. [2016a] "High-flexibility, high-toughness double-cross-linked chitin hydrogels by sequential chemical and physical cross-linkings," *Advanced Materials* **28**(28), 5844–5849.

Xu, S., Cai, S. and Liu, Z. [2018] "Thermal conductivity of polyacrylamide hydrogels at the nanoscale," *ACS Applied Materials and Interfaces* **10**(42), 36352–36360.

Xu, S. and Liu, Z. [2019] "A nonequilibrium thermodynamics approach to the transient properties of hydrogels," *Journal of the Mechanics and Physics of Solids* **127**, 94–110.

Xu, S., Wang, Y., Hu, J. and Liu, Z. [2016b] "Atomic understanding of the swelling and phase transition of polyacrylamide hydrogel," *International Journal of Applied Mechanics* **8**(7), 1640002.

Xu, W. and Li, G. [2010] "Constitutive modeling of shape memory polymer based self-healing syntactic foam," *International Journal of Solids and Structures* **47**(9), 1306–1316.

Yang, J., Bai, R., Chen, B. and Suo, Z. [2019] "Hydrogel adhesion: A supramolecular synergy of chemistry, topology, and mechanics," *Advanced Functional Materials*, Vol. 1901693.

Yang, Q. and Li, G. [2015] "Temperature and rate dependent thermomechanical modeling of shape memory polymers with physics based phase evolution law," *International Journal of Plasticity* **80**, 168–186.

Yu, Y., Landis, C. M. and Huang, R. [2017] "Salt-induced swelling and volume phase transition of polyelectrolyte gels," *Journal of Applied Mechanics* **84**(5), 051005–051012.

Zeng, H., Leng, J. S., Gu, J. P. and Sun, H. Y. [2018] "A thermoviscoelastic model incorporated with uncoupled structural and stress relaxation mechanisms for amorphous shape memory polymers," *Mechanics of Materials* **124**, 18–25.

Zhang, N., Pan, Z., Lei, J. and Liu, Z. [2018a] "Effects of temperature on the fracture and fatigue damage of temperature sensitive hydrogels," *RSC Advances* **8**(54), 31048–31054.

Zhang, N., Zheng, S., Pan, Z. and Liu, Z. [2018b] "Phase transition effects on mechanical properties of nipa hydrogel," *Polymers* **10**(4), 358.

Zhang, Y., Chen, L., Swaddiwudhipong, S. and Liu, Z. [2014] "buckling deformation of annular plates describing natural forms," *International Journal of Structural Stability and Dynamics* **14**(1), 1350054.

Zhang, Y., Liu, Z., Swaddiwudhipong, S., Miao, H., Ding, Z. and Yang, Z. [2012] "pH-sensitive hydrogel for micro-fluidic valve," *Journal of Function Biomater* **3**(3), 464–479.

Zhao, R., Kim, Y., Chester, S. A., Sharma, P. and Zhao, X. [2019] "Mechanics of hard-magnetic soft materials," *Journal of the Mechanics and Physics of Solids* **124**, 244–263.

Zheng, S. and Liu, Z. [2019] "Constitutive model of salt concentration-sensitive hydrogel," *Mechanics of Materials* **136**, 103092.

Zhong, D., Xiang, Y., Yin, T., Yu, H., Qu, S. and Yang, W. [2019] "A physically-based damage model for soft elastomeric materials with anisotropic Mullins effect," *International Journal of Solids and Structures* **176–177**, 121–134.

Zhou, Y., Hu, J. and Liu, Z. [2019] "Deformation behavior of fiber-reinforced hydrogel structures," *International Journal of Structural Stability and Dynamics* **19**(3), 1950032.